NASA CR-179563

HSER 10853

Expansion of Epicyclic Gear Dynamic Analysis Program

(NASA-CR-179563) EXPANSION OF EPICYCLIC GEAR DYNAMIC ANALYSIS PROGRAM Final Report (Hamilton Standard, Windsor Locks, Conn.) 94 p CSCL 13I N87-19723 Unclas G3/37 43521

Final Report

by

Linda Smith Boyd

and

James Pike

Hamilton Standard
Division of United Technologies Corporation
Windsor Locks, CT. 06096

Prepared for

National Aeronautics and Space Administration
NASA Lewis Research Center
Contract NAS3-24614

NASA CR-179563

HSER 10853

Expansion of Epicyclic Gear Dynamic Analysis Program

Final Report

by

Linda Smith Boyd

and

James Pike

Hamilton Standard
Division of United Technologies Corporation
Windsor Locks, CT. 06096

Prepared for

National Aeronautics and Space Administration
NASA Lewis Research Center
Contract NAS3-24614

1. Report No.	2. Government Accession No.	3. Recipient's Catalog No.
CR 179563		

4. Title and Subtitle	5. Report Date
Expansion of Epicyclic Gear Dynamic Analysis Program	August, 1986
	6. Performing Organization Code: 505-63-51
7. Author(s): L. S. Boyd and J. A. Pike	8. Performing Organization Report No.
	10. Work Unit No.
9. Performing Organization Name and Address: Hamilton Standard Division of United Technologies Windsor Locks, CT. 06096	11. Contract or Grant No.: NAS3-24614
12. Sponsoring Agency Name and Address: NASA Lewis Research Center Cleveland, OHIO	13. Type of Report and Period Covered: Contractor Report
	14. Sponsoring Agency Code

15. Supplementary Notes

Dennis Townsend, Project Manager
NASA Lewis Research Center
21000 Brookpark Road
Cleveland, OHIO 44135

16. Abstract

The multiple mesh/single stage dynamics program is a gear tooth analysis program which determines detailed geometry, dynamic loads, stresses and surface damage factors. The program can analyze a variety of both epicyclic and single mesh systems with spur or helical gear teeth including internal, external, and buttress tooth forms.

The modifications refine the options for the flexible carrier and flexible ring gear rim and adds three new options: a floating sun gear option, a natural frequencies option, and a finite element compliance formulation for helical gear teeth. The option for a floating sun incorporates two additional degrees of freedom at the sun center. The natural frequency option evaluates planetary, star or differential systems' frequencies as well as the effect of additional springs at the sun center and those due to a flexible carrier and/or ring gear rim. The helical tooth pair calculated finite element compliance is obtained from an automated element breakup of the helical teeth and then is used with the basic gear dynamic solution and stress postprocessing routines. The flexible carrier or ring gear rim option for planetary and star spur gear systems allows the output torque per carrier and ring gear rim segment to vary based on the dynamic response of the entire system, while the total output torque remains constant.

17. Key Words (Suggested by Author(s))	18. Distribution Statement
Gear tooth dynamic stresses floating sun, gear tooth frequencies, helical teeth	Unclassified - Unlimited

19. Security Classif. (of this report)	20. Security Classif. (of this page)	21. No. of Pages	22. Price*
Unclassified	Unclassified		

* For sale by the National Technical Information Service, Springfield, Virginia 22161

NASA-C-168 (Rev. 10-75)

ABSTRACT

The multiple mesh/single stage dynamics program is a gear tooth analysis program which determines detailed geometry, dynamic loads, stresses and surface damage factors. The program can analyze a variety of both epicyclic and single mesh systems with spur or helical gear teeth including internal, external, and buttress tooth forms.

The modifications refine the options for the flexible carrier and flexible ring gear rim and adds three new options: a floating sun gear option, a natural frequency option, and a finite element compliance formulation for helical gear teeth. The option for a floating sun incorporates two additional degrees of freedom at the sun center. The natural frequency option evaluates the frequencies of planetary, star or differential systems as well as the effect of additional springs at the sun center and those due to a flexible carrier and/or ring gear rim. The helical tooth pair finite element calculated compliance is obtained from an automated element breakup of the helical teeth and then is used with the basic gear dynamic solution and stress postprocessing routines. The flexible carrier or ring gear rim option for planetary and star spur gear systems allows the output torque per carrier and ring gear rim segment to vary based on the dynamic response of the entire system, while the total output torque remains constant.

TABLE OF CONTENTS

LIST OF FIGURES

NASA CR-179563
HSER 10853

Expansion of Epicyclic Gear Dynamic Analysis Program

Final Report

by

Linda Smith Boyd

and

James Pike

Hamilton Standard
Division of United Technologies Corporation
Windsor Locks, CT. 06096

Prepared for

National Aeronautics and Space Administration
NASA Lewis Research Center
Contract NAS3-24614

1. Report No. CR 179563	2. Government Accession No.	3. Recipient's Catalog No.
4. Title and Subtitle Expansion of Epicyclic Gear Dynamic Analysis Program		5. Report Date August, 1986 6. Performing Organization Code 505-63-51
7. Author(s) L. S. Boyd and J. A. Pike		8. Performing Organization Report No. 10. Work Unit No.
9. Performing Organization Name and Address Hamilton Standard Division of United Technologies Windsor Locks, CT. 06096		11. Contract or Grant No. NAS3-24614 13. Type of Report and Period Covered Contractor Report
12. Sponsoring Agency Name and Address NASA Lewis Research Center Cleveland, OHIO		14. Sponsoring Agency Code

15. Supplementary Notes

Dennis Townsend, Project Manager
NASA Lewis Research Center
21000 Brookpark Road
Cleveland, OHIO 44135

16. Abstract

The multiple mesh/single stage dynamics program is a gear tooth analysis program which determines detailed geometry, dynamic loads, stresses and surface damage factors. The program can analyze a variety of both epicyclic and single mesh systems with spur or helical gear teeth including internal, external, and buttress tooth forms.

The modifications refine the options for the flexible carrier and flexible ring gear rim and adds three new options: a floating sun gear option, a natural frequencies option, and a finite element compliance formulation for helical gear teeth. The option for a floating sun incorporates two additional degrees of freedom at the sun center. The natural frequency option evaluates planetary, star or differential systems' frequencies as well as the effect of additional springs at the sun center and those due to a flexible carrier and/or ring gear rim. The helical tooth pair calculated finite element compliance is obtained from an automated element breakup of the helical teeth and then is used with the basic gear dynamic solution and stress postprocessing routines. The flexible carrier or ring gear rim option for planetary and star spur gear systems allows the output torque per carrier and ring gear rim segment to vary based on the dynamic response of the entire system, while the total output torque remains constant.

17. Key Words (Suggested by Author(s)) Gear tooth dynamic stresses floating sun, gear tooth frequencies, helical teeth	18. Distribution Statement Unclassified - Unlimited

19. Security Classif. (of this report) Unclassified	20. Security Classif. (of this page) Unclassified	21. No. of Pages	22. Price*

* For sale by the National Technical Information Service, Springfield, Virginia 22161

NASA-C-168 (Rev. 10-75)

ABSTRACT

The multiple mesh/single stage dynamics program is a gear tooth analysis program which determines detailed geometry, dynamic loads, stresses and surface damage factors. The program can analyze a variety of both epicyclic and single mesh systems with spur or helical gear teeth including internal, external, and buttress tooth forms.

The modifications refine the options for the flexible carrier and flexible ring gear rim and adds three new options: a floating sun gear option, a natural frequency option, and a finite element compliance formulation for helical gear teeth. The option for a floating sun incorporates two additional degrees of freedom at the sun center. The natural frequency option evaluates the frequencies of planetary, star or differential systems as well as the effect of additional springs at the sun center and those due to a flexible carrier and/or ring gear rim. The helical tooth pair finite element calculated compliance is obtained from an automated element breakup of the helical teeth and then is used with the basic gear dynamic solution and stress postprocessing routines. The flexible carrier or ring gear rim option for planetary and star spur gear systems allows the output torque per carrier and ring gear rim segment to vary based on the dynamic response of the entire system, while the total output torque remains constant.

TABLE OF CONTENTS

LIST OF FIGURES

LIST OF TABLES

I. SUMMARY

The epicyclic gear program is a multiple mesh/single stage, gear dynamics program. It is a versatile gear tooth dynamic analysis computer program which determines detailed geometry, dynamic loads, stresses and surface damage factors. The program can analyze a variety of both epicyclic and single mesh systems with spur and helical gear teeth including internal, external, and buttress tooth forms. This NASA Lewis sponsored contract called for four improvements: refinement of the option for the flexible carrier or flexible ring gear rim, a floating sun gear option, a natural frequencies option, and a finite element compliance formulation for helical gear teeth.

Task I was to add an option for a floating sun to account for flexible sun gear mounting, which incorporates two additional degrees of freedom at the sun center. Generally, soft mounted sun gears are used to minimize the effects of gear runout, etc. The test case used for the program checkout was a lightly loaded, three planet, planetary system. The floating sun case results showed similar loads for the sun-planet meshes and slightly higher loads for the ring-planet meshes when compared to the rigidly mounted sun case. Other cases, with higher loads and various spring rates, should be examined to analyze the effect more thoroughly.

Task II was to add an option to determine the natural frequencies of the system. This option is desirable to predict system critical speeds without having to run the complete dynamic analysis for a range of input speeds. The information can also aid the user in running the dynamic solution routines. At the system critical speeds the dynamic loads will be much more sensitive to the input variables and the user will know where these speeds occur beforehand. Planetary, star or differential systems can be investigated as well as the effect of the additional springs at the sun center (floating sun) and those due to a flexible carrier and/or ring gear rim. In addition, the effect of variation of the tooth pair stiffness on the natural frequencies due to load position can be investigated. The frequency results are consistent with the program's dynamic response solution.

Task III was to generate a helical tooth compliance routine based on finite element modeling. The previous version divided the tooth into ten equivalent spur gear teeth and used the spur tooth routines for the dynamic solution. However, this technique did not allow for coupling between the equivalent spur teeth segments. The program also had provisions to input a general compliance matrix for the helical gear tooth to be analyzed, but the user had to know the matrix before running the gear dynamics program. This added finite element routine eliminates these prior shortcomings. The new option internally generates a finite element breakup of the helical teeth and the necessary data for the internal finite

element routines. The routines use a four noded, quadrilateral, higher order plate element with five degrees of freedom per node. The results are used to obtain a general tooth pair compliance curve which is then used by the basic dynamic solution routines.

Task IV was to refine the flexible carrier and ring gear rim options for planetary and star spur gear systems. The frequency equations were expanded to account for nonrigid carriers and ring gear rims. In addition, some minor modifications were made with respect to the numerical solution tolerances. These modifications results in more stable solutions, thus allowing the user to investigate the effects of various spring rates for both the carrier and the carrier/planet pin, eg. a bearing, or for the ring gear rim and the corresponding pin.

II. INTRODUCTION

A. PROGRAM HISTORY

The multiple mesh gear dynamic analysis computer code has been under development at Hamilton Standard for about five years. The program can determine detailed geometry, dynamic loads, stresses, and surface damage factors for epicyclic gear systems and single mesh systems with internal, external, buttress, or helical tooth forms. The significant parameters can be plotted through the entire mesh in addition to the maximum values which are tabulated as output from the program.

The initial program, a single spur gear mesh, was written for high contact as well as low contact ratio gearing. The basic concept was an extension of that developed by Richardson in 1958. Since the basic program was developed, many enhancements and refinements have been made. Buttress, internal and external involute tooth forms can be analyzed for spur and helical gear teeth. Tooth spacing errors, runout errors, involute profile modifications, etc. can be accounted for in the dynamic solution.

The program has been developed to operate over a wide range of contact ratios, and to allow the gear teeth to have a different pressure angle on the drive side and coast side (buttress form). The teeth of the meshes being analyzed may have modified profiles and spacing errors may be specified. Influence coefficients may be input for rim and web geometry to determine the effect on peak dynamic stress caused by non-uniform stiffness along the width of the gear, dependent on the design configuration of the foundation under the gear tooth. More recent additions to the program include variable contact friction throughout each mesh, user friendly options, dynamic side bands, a speed survey option and the option of solving non-planetary or single mesh systems. See References 1 through 6 for more details.

B. PROGRAM ENHANCEMENTS

This NASA contract refines the option for the flexible carrier or flexible ring gear rim and adds three new options: a floating sun gear option, a natural frequency option, and a finite element compliance formulation for helical gear teeth.

Task I was to add an option to allow the sun to float at the center. This allows for investigation of the effects of different spring rates and damping at the sun center on the dynamic tooth load behavior. This was accomplished by adding two global translational degrees of freedom at the sun center. These translational degrees of freedom were transformed into degrees of freedom along the respective meshing lines of action, to remain consistent with the existing code. The theoretical development was aided by the work of Hidaka et al, Reference 7.

Task II was to develop a routine for calculating the natural frequencies of the gear system. This was accomplished by solving the classical eigenvalue problem. This option will solve for the frequencies of the system using tooth pair compliances at the pitch diameter. The designer can also utilize the load position varying gear tooth compliance formulation and evaluate the frequencies at other mesh positions. This option allows the user to investigate the effects of different spring rates and masses throughout the gear system on the critical speeds.

Task III was to refine the helical gear tooth compliance routines. The refinement was to incorporate convective (coupled) compliance effects which were not previously included. This involved adding routines to build finite element models of the helical gear teeth, Reference 8. The models are used to obtain a spur gear compliance formulation which utilizes the basic gear dynamic routines and stress postprocessors. This refined approach uses much less CPU time, as well as using a smaller time step for the numerical solution, which will lead to a more stable dynamic solution than the previous uncoupled spur tooth segment approach. However, for helical gears with large helix angles the stress postprocessing will give unconservative results.

Task IV was to refine the flexible carrier/ring gear rim option. This option allows the user to investigate the effects of various stiffnesses for the carrier or ring gear rim as well as the pin stiffness between the planet gear and the carrier or the ring gear rim and the output shaft. This involved investigation of previous work, Reference 1, in order to determine the cause of an instability. The numerical solution technique was evaluated, as well as review of the mathematical model. The most significant change was in the mathematical model, where the forcing functions of the carrier or ring gear segment equations were modified to vary with respect to time while the total output torque remained constant. In addition, some minor changes were made to the numerical solution parameters to increase stability.

These four improvements further enhance the flexibility of the multiple mesh gear dynamics program and the variety of applications that can be modeled. The modifications allow the user to investigate a wider variety of system complexities. For example, a simple planetary can now be evaluated utilizing various additional degrees of freedom such as the floating sun gear or the flexible carrier, which are likely to be influential in a real system. The finite element compliance formulation lays the groundwork for a more exact modeling of the helical gear teeth.

III. FLOATING SUN GEAR

A. PROGRAM MODIFICATIONS

The floating sun gear option adds two additional degrees of freedom at the sun center. Springrates are required for the two orthogonal directions at the sun center as well as the translational mass of the sun gear and the additional boundary conditions. The equations of motion for the sun center are included in the system of equations being solved.

The equations of motion for the sun gear center in Cartesian coodinates, x and y directions, using the model of Figure 1, can be written:

$$m_s\ddot{x} + d_x\dot{x} + k_x x - \sum_{i=1}^{N} d_{sp_i}\dot{y}_{sp_i}\sin\alpha_i - \sum_{i=1}^{N} L_{sp_i}\sin\alpha_i = 0 \tag{1}$$

$$m_s\ddot{y} + d_y\dot{y} + k_y y + \sum_{i=1}^{N} d_{sp_i}\dot{y}_{sp_i}\cos\alpha_i + \sum_{i=1}^{N} L_{sp_i}\cos\alpha_i = 0 \tag{2}$$

where $\alpha_i = \theta_c + \Psi_i - \Phi$ (planetary)

$\alpha_i = \Psi_i - \Phi - \theta_r$ (star)

The angle, α_i, is for resolution of the tooth pair forces from along the line of action to the Cartesian coordinates, x and y. The pressure angle, Φ, was assumed to remain constant through the mesh; however, the more precise formulation would account for the varying angle at different mesh times. It is believed this assumption has secondary effects on the results. However, the information is available in the code such that the varying angle could be included during future enhancements.

In addition to the sun center equations, the carrier or ring rotational displacements, corresponding to a planetary or star system respectively, are also required to obtain the angle, α. Thus the following equations must also be solved for a rigid carrier or rigid ring gear rim in conjunction with the tooth pair mesh equations, Reference 2, and equations (1) and (2).

$$m_c \ddot{y}_c - \sum_{i=1}^{N} d_{sp_i} \dot{y}_{sp_i} - \sum_{i=1}^{N} d_{rp_i} \dot{y}_{rp_i}$$

$$- \sum_{i=1}^{N} L_{sp_i} - \sum_{i=1}^{N} L_{rp_i} = F_c$$

where: $F_c = - \tau_{out}/R_{b_c}$ (planetary)

$F_c = 0$ (star) (3)

$y_c = R_{b_c} \theta_c$

$$m_r \ddot{y}_r - \sum_{i=1}^{N} d_{rp_i} \dot{y}_{rp_i} - \sum_{i=1}^{N} L_{rp_i} = F_r$$

where: $F_r = 0$ (planetary)

(4)

$F_r = - \tau_{out}/R_{b_r}$ (star)

$y_r = R_{b_r} \theta_r$

The numerical solution requires these equations be reduced to first order differential equations; thus equations (1), (2), and (3) or (4) are added to the system of equations via six first order equations, see Appendix B.

The sun center displacements must be resolved in the direction of the line of action to determine the effect on the tooth pair meshes. This is accomplished via:

$$x_{LOA_i} = y \cos \alpha_i - x \sin \alpha_i \tag{5}$$

The tooth pair meshing loads of Reference 2, then become:

$$L_{sp_i} = \sum_{j=1}^{m} [(y_{sp_i} - e_{sp_{ji}} - \chi^2{}_{sp_{ji}} \beta^2{}_{sp_{ji}} + x_{LOA_i})\eta_{sp_{ji}} \phi_{sp_{ji}}] \tag{6a}$$

$$L_{rp_i} = \sum_{j=1}^{m} [(y_{rp_i} - e_{rp_{ji}} - \chi^2{}_{rp_{ji}} \beta^2{}_{rp_{ji}})\eta_{rp_{ji}} \phi_{rp_{ji}}] \tag{6b}$$

where m is the number of teeth in contact at mesh i, η_{sp_i} is the tooth pair stiffness and ϕ_{sp_i} is a tooth pair contact identity function.

To obtain a steady state solution, the solution is iterated until the boundary conditions converge for the tooth pair meshes. Convergence is determined by comparing the displacements along the lines of action due to the sun center movement to the largest sun-planet tooth pair displacement. Convergence is faster when the spring rates at the sun center are of similar order of magnitude to the tooth pair stiffnesses.

B. DISCUSSION OF FLOATING SUN RESULTS

The addition of the floating sun gear option allows the user to analyze various sun center spring rates and damping and the resulting dynamic tooth loads. Most epicyclic gear systems have a sun gear that can move in the in-plane translational directions, thus this option incorporates degrees of freedom that are of practical interest.

Two test cases were run using a lightly loaded planetary gear system. The description of the spur gear test case, Task I, Example 1.1, is described in Table 1 and was run using both the three planets of the system and reducing the number of planets to two. Several spring rates at the sun center were examined. The results for the three planet cases are summarized in Table 2.

The three planet cases included phasing constants to account for the different location of each planet mesh on its respective line of action. Because of the interactive dynamics, the total distances moved along the lines of action, due to the additional sun center movement, can be different for each mesh. In the three planet case with sun center springs 4.4 times the sun-planet tooth pair stiffness (10,000,000 lb./in. and damping of 5 %) the maximum loads increased from 2 to 7 percent for the sun-planet loads and from 14 to 15% for the ring-planet meshes. The ring-planet meshes also indicated a decrease in the dynamic contact ratio, which is calculated by determining the total tooth contact time for one tooth pass during the dynamic solution. A low dynamic contact ratio represents tooth pair separation, which indicates tooth bouncing may be occurring, possibly causing the load increase. The additional degrees of freedom at the sun center may have introduced natural frequencies near the operating speed which could also cause the load increase.

The sun center spring rates were increased to 30,000,000 lb/in, or 13 times the sun-planet tooth pair stiffness. The no tooth error case showed the sun-planet loads less than 3 % different and the ring-planet loads were generally a little higher, 4-5 %, for 2 % damping. Thus, as the springs become stiffer, the loads approach the non-flexible sun center mount solution as expected.

The two planet case showed no variation in the maximum tooth pair loads. As expected, the diametrally opposed planets (equal phasing constants) moved in equal and opposite directions along their lines of action due to equal tooth pair stiffnesses. The two cases executed to confirm these results were for sun center spring rates of 300,000 lb/in and 30,000 lb/in. Both cases yielded results identical to the non-floating sun gear.

IV. NATURAL FREQUENCY OPTION

A. PROGRAM MODIFICATIONS

The natural frequency option allows the user to investigate natural frequencies of the system through a classical eigenvalue solution. The effects of various spring rates at the sun center for a floating sun, or the effect of various stiffnesses of a planet carrier and/or ring gear rim on the frequency response can readily be determined. In addition, by using the planet phasing constants, the range of frequencies due to the nonlinear tooth meshing action can be investigated.

The general form of the dynamic equations for the eigenvalue solution is:

$$[M]\{\ddot{x}\} + [K]\{x\} = 0 \qquad (7)$$

The mass and stiffness matrices [M] and [K], are derived from the system of equations of References 1 and 2, as well as equations (1) to (4). The eigenvector/eigenvalue solution, which assumes harmonic motion, then solves for the roots of the determinant:

$$\left| [K] - \lambda [M] \right| = 0 \qquad (8)$$

A standard eigenvalue/eigenvector numerical solution routine for real, symmetric matrices was used to solve the determinant, Reference 9.

The program also calculates the gear mesh frequencies using the following equation.

$$f_I = rpm/60. * XN * I \qquad I = 1, 2, 3 \ldots \qquad (9)$$

These gear mesh frequencies are printed with the natural frequencies to aid the user in generating critical speed diagrams.

The natural frequency option can be used for eight system types: planetary, star, differential, single meshes, planetary with flexible carrier, star with flexible ring gear rim, or a differential system with both a flexible ring gear rim and a flexible planet carrier. In addition, the floating sun degrees of freedom can be included in the natural frequency solution.

This option is initiated by a trigger with two choices of output format, either natural frequencies and gear mesh frequencies or full output which also includes the eigenvectors. After the frequencies have been calculated, the program ends and does not continue with the dynamic load solution.

The frequency solution uses tooth pair stiffnesses from the nonlinear compliance formulation of the gear program, Reference 4 and 5. This compliance formulation also includes the Hertzian effect; thus, the torque that is input will influence the natural frequencies. A zero torque case will eliminate the Hertzian effect if it is not desired.

The natural frequency solution is for a specific instant in time, with the corresponding tooth pair stiffnesses. If no phasing constants are included, the tooth pair stiffnesses will be those at the pitch diameter. The phasing constants can be used to simulate different times and therefore different stiffnesses in the mesh. These phasing constants tell the program that the different planet meshes are at different positions with respect to each other along their lines of action. This indicates that all the planet meshes may not be at the pitch diameter initially. See User's Manual for details on calculation of the phasing constants.

B. DISCUSSION OF NATURAL FREQUENCY RESULTS

The natural frequency option is a useful tool for predicting critical speeds. This option allows for investigation of the effect of mesh position dependent tooth pair stiffnesses on the natural frequencies, as well as the additional frequencies due to carrier and ring flexibilities and floating sun flexibilities. The eigenvalue/eigenvector solution executes rapidly, as the program does not continue with the dynamic load solution. Thus, this is an economical approach to investigate the effects of various spring rates or masses on the natural frequencies.

The natural frequency option can be used to calculate the speed ranges where high dynamic loads could occur. This can also assist the user in reducing the number of boundary condition iterations that are necessary for convergence for a regular dynamic load solution by avoiding these critical speed areas. The effects of different spring rates throughout the gear system on the critical speeds can also be investigated. It also allows the designer to increase the number of degrees of freedom and observe the additional frequencies. For example, a simple planetary system will have N + 2 degrees of freedom, where N is the number of planets. The designer can add two spring rates at the sun center for N + 4 degrees of freedom, then could increase the total degrees of freedom again to 2N + 4 via the carrier flexibility.

Several test cases were run,and two examples are presented in Figures 3 and 4. Both figures show the critical speeds predicted by the natural frequency option, and the critical speeds predicted by running speed surveys with the dynamic response solution, Reference 1. Both cases agree in predicting the natural frequencies when the pitch diameter tooth pair stiffnesses were used for the eigenvalue solution.

Figure 3 shows a critical speed diagram for Example 2.1, Table 1, and Figure 4 shows Example 2.2. The horizontal bands illustrate the range of frequencies that result from the variation of tooth pair stiffnesses through the mesh. The variation in frequency due to tooth pair stiffnesses versus percent of total mesh positions is shown in Figure 5 and corresponds to Figure 3. The higher frequencies of the band are when the mesh is at the pitch diameter and the tooth pair stiffness is maximum. The lower frequencies of the bands are at other positions in the mesh. These were simulated by adjusting the planet phasing constants until the minimum stiffness for the sun-planet meshes and the minimum stiffness for the ring-planet meshes were obtained.

The case in Figure 3 showed reasonable correlation between the natural frequency option and the results of an analytical speed survey using the dynamic solution. This was a two planet case with unequal phasing. The speed survey response results indicated peak dynamic loads in the range of sun gear input speeds of 23,000 to 25,000 rpm, a distinct peak near 7,000 rpm and a smaller load increase near 12,000 rpm. This case was previously shown to have reasonable correlation to test data, Reference 1.

By varying the stiffnesses the frequencies can be easily associated with particular degrees of freedom; e.g., in Example 2.2, when the sun-planet stiffness decreased significantly, the highest frequency decreased and when the ring-planet stiffness decreased, the two lower frequencies decreased. Thus, the highest of the gear mesh frequencies is due to the sun-planet meshes, while the lower frequencies are due to the ring-planet meshes. This may not be immediately obvious from the eigenvectors, because they indicate the motion along the lines of action for each gear and not the relative motion of the sun-planet or ring-planet meshes.

For planetary, star, and differential systems, the carrier and/or ring gear are treated as rigid bodies, unless the flexible carrier or flexible ring gear rim options are selected. The rigidity is also evident in the resulting natural frequencies. The eigenvalue solution yields one rigid body mode for planetary and star systems corresponding to the rigid carrier or ring gear, and the differential system results in two rigid body modes corresponding to both the rigid carrier and ring gear. These rigid body modes are not shown in the table of natural frequencies; however, if the user requests full output, all of the frequencies are printed as well as the mass and stiffness matrices and all eigenvectors.

Systems with a flexible carrier and/or ring gear rim may yield rigid body modes if the stiffnesses of the carrier and/or ring gear rim or pin stiffnesses are relatively high. For these situations, either the carrier and/or the ring are acting as rigid bodies. For these systems all the frequencies are output, but if the first two modes are orders of magnitude less than the other frequencies, the pin stiffnesses and/or the program results should be carefully examined.

V. REFINED HELICAL COMPLIANCE ROUTINES

A. PROGRAM MODIFICATIONS

An option for helical gear analysis was added which incorporates a finite element analysis to obtain a tooth pair compliance curve. Several new subroutines have been added to the code to generate finite element models of the helical gear teeth. These models are then used to calculate tooth pair compliance curves. The model generation is internal to the code, so the user need only input an additional trigger to initiate the option.

The finite element option uses two finite element plate routines, Reference 8, to generate the stiffnesses for both in-plane and out-of-plane loads, as well as a routine to process the information to and from the multiple mesh program . Figure 6 summarizes the procedure via a flow chart.

For both routines, four noded isoparametric plate elements, with a total of five degrees of freedom per node, are used. The routine for out-of-plane loads includes transverse shear effects. The model for any tooth will have 9 elements along the face width and 9 elements along the tooth centerline (10 by 10 nodes), see Figure 7. The plate thicknesses are average thicknesses determined from the existing tooth geometry subroutines.

The tooth model is fixed at the root and displacements are applied along seven equally spaced load lines via boundary conditions for the finite element solution. The reaction forces along the load lines are used in conjunction with the applied displacements to obtain average stiffnesses for seven load line positions.

The existing spur tooth pair compliance used in the program includes axial bending, Hertzian, and fillet and foundation effects, Reference 5 and 6. These are determined for seven load positions for each tooth pair and combined to obtain total compliances. A curve fitting routine is then used to obtain the following fourth order polynomial for compliance as a function of position along the line of action.

$$C = C_0 \left[1 + A(S/S_0) + B(S/S_0)^2 + C(S/S_0)^3 + D(S/S_0)^4 \right] \qquad (10)$$

The finite element model accounts for the axial bending and fillet effects and an average Hertzian effect. The load line position at the center of the helical tooth face width is used to calculate an average Hertzian compliance.

This approach accounts for the helix angle, but uses the spur gear dynamic solution technique. The previous helical solution divided the tooth into ten equivalent spur gear tooth segments. Each of the segments was evaluated dynamically and the CPU running time was quite long to solve for each segment at each of 100 time steps. Because of this, the number of time steps had been reduced to ten for the previous helical solution. However, because the finite element approach is more direct than the segment approach, the time step was increased back to 100 for this option to improve the accuracey and response definition.

B. DISCUSSION OF REFINED HELICAL GEAR COMPLIANCE RESULTS

This option offers the user an alternative helical gear tooth analysis. A compliance curve was generated using the existing formulations for Hertzian effects and detailed geometry to obtain plate thicknesses to be used with two finite element routines, one for in-plane loads and one for out-of-plane loads, see Figure 8 for example output of Task III, Example 3.1, Table 1.

Future improvements should include further refinement of the stress postprocessing, where the finite element routines could be utilized more fully. The current finite element configuration utilizes the spur gear stress postprocessing routines by using the calculated dynamic load and applying it to the center of the tooth face width. This could lead to unconservative stress results when the helix angle is large, because the load line is parallel to the axis of rotation for spur gear postprocessing. A more complete solution would utilize the flexibility matrix generated by the finite element routines in conjunction with the dynamic solution. This more precise method would involve calling the finite element routines directly during the dynamic solution, which would require significant amounts of additional computer time. Similarly, finite element stress sensitivity routines that use the plate element directly for postprocessing could be included.

The number of elements that are chosen for the mesh breakup should be changed to be a user input in future work. The current constant breakup could lead to width to height ratios that exceed acceptable limits for finite element aspect ratios for wide teeth. The tooth fillet elements could also be refined. It was assumed that the first row of elements would extend from the root to the first point of contact, while the plate thicknesses were modified to estimate the additional fillet material, see Figure 9. However, this does not accurately define this area and could lead to significant element size variation and therefore error for cases with large fillet radii relative to the tooth height.

VI. FLEXIBLE CARRIER EVALUATION

A. PROGRAM MODIFICATIONS

During the previous contract work (CR # 174747) an attempt had been made to add the flexible carrier option to the dynamics model. However, numerical instabilities had occurred in the check case solutions which were not resolved during that contract. Therefore, the flexible carrier/ring gear rim dynamic solutions were reviewed with respect to the numerical solution, the equations, and the FORTRAN code. The major improvement was to the output torque term of the flexible carrier or flexible ring gear equations, i.e. the forcing function for the differential equation. This term was modified to calculate the output torque from the carrier or ring segment displacements and an interface stiffness, such as a pin or bearing stiffness, while the total output torque was constrained to remain constant.

The theoretical model is shown in Figure 10, and can be used to write the carrier or ring segment equations of motion as follows.

$$\begin{aligned} & m_{c_i}\ddot{Y}_{c_i} - d_{sp_i}(\dot{Y}_s - \dot{Y}_{p_i} - \dot{Y}_{c_i}) - d_{rp_i}(\dot{Y}_{p_i} - \dot{Y}_{c_i} - \dot{Y}_{r_i}) \\ & - L_{sp_i} - L_{rp_i} + K_{c_i}(Y_{c_i} - Y_{c_{i+1}}) \\ & + K_{c_{i-1}}(-Y_{c_{i-1}} + Y_{c_i}) = - \bar{K}_c\, Y_{c_i} \end{aligned} \qquad (11)$$

$$\begin{aligned} & M_{r_i}\ddot{Y}_{r_i} - d_{rp_i}(\dot{Y}_{p_i} - \dot{Y}_{c_i} - \dot{Y}_{r_i}) - L_{rp_i} \\ & + K_{r_{i-1}}(-Y_{r_{i-1}} + Y_{r_i}) + K_{r_i}(Y_{r_i} - Y_{r_{i+1}}) = - \bar{K}_r Y_{r_i} \end{aligned} \qquad (12)$$

and $$\sum_{i=1}^{N} \bar{K}_c Y_{c_i} = \tau_{out} / R_b \,. \qquad (13)$$

Equation (13) adds one more equation than there are unknowns; thus, a constraint must be simulated in the numerical solution routines by introducing another parameter. The numerical routine used to solve the system of first order equations does not have the direct capability of a constraint on a primary variable, i.e. Y_{ci}. Therefore, an artificial mass which simulates a large inertia, assumed to be 1000 times the largest mass of the system and attached to the carrier or ring, was added to the system of equations. This results in $\ddot{x} = 0$, analogous to the system shown in Figure 12. The additional equation of motion is:

$$M\ddot{X} + \sum_{i=1}^{N} \bar{K}_{c_i} Y_{c_i} = \tau_{out}/R_{b_c} \qquad \text{(14) (carrier)}$$

or:

$$\overline{M}\,\ddot{X} + \sum_{i=1}^{N} \overline{K}_{r_i} Y_{r_i} = \tau_{out}/R_{b_r} \qquad \text{(15) (ring)}$$

This increases the number of second order equations by 1 to (3N + 2). The first order equations used for the numerical solution are in Appendix B.

The numerical solution routine was also investigated with respect to stability. A simple example was used in conjunction with the numerical solution routines to determine the effect of the size of the integration time steps on the solution. The example used a system of differential equations similar to the equations for a planetary system. They were used directly in the numerical solution routines, independent of the gear program. It was verified that the time step used for the numerical integration could lead to erroneous results if the step size was too large. This step size was previously a constant value in the multiple mesh code, but the total mesh time varies for different systems. A better choice for the integration time step is a function of the meshing time. Therefore, the integration time step was then changed to be 0.001 percent of the time for each mesh cycle.

This step size change can actually reduce the number of iterations internal to the numerical routines, due to the way the solution routine handles the step size if it is too large. If the routine is given a step size that is too large, it reduces the integration step size and tries again until it is small enough to yield a good solution. If it is given a step size that is adequate initially, it will obtain a good solution more rapidly. As this occurs for each of the 100 time steps in the dynamic solution, this could lead to significant reductions in computation time for some cases.

The size of the mesh time step can also have an effect on the solution. This is currently set to be equal to the total mesh time divided by 100. For very low speeds this time step can become relatively large and could lead to an unstable solution.

B. DISCUSSION OF FLEXIBLE CARRIER RESULTS

The flexible carrier modifications allow the user to investigate the effect of a carrier with additional flexibility, along the line of action, on the dynamic tooth loads of a spur gear system. Similarly, additional flexiblity in the ring gear rim along the line of action. Two test cases with different carrier stiffnesses for a planetary spur system (flexible carrier) were investigated. They indicated higher maximum loads for the more flexible systems. This is due to the increased tooth pair bouncing that occurred, as was indicated by lower dynamic contact ratios.

Figures 12a and 12b illustrate the non-flexible test case numerical results and a case, Example 4.1, Task IV, Table 1, with a pin stiffness of 2,500,000 lbs/in. and a carrier stiffness of 5,000,000 lbs/in. The maximum tooth loads increased with the increased flexibility of the planet carrier. For this case, the ring-planet loads increased more than the sun-planet loads, 12.5% and 5.9%. Results from another case, with equal carrier and pin spring rates showed that the sun-planet mesh loads increased 9.3%, while the ring-planet loads increased by 5.4%.

Figures 13a and 13b show the plots generated by the multiple mesh program for the first planet mesh for the nonflexible case and for the case with pin stiffness of 2,500,000 lbs/in., respectively. There were no planet phasing constants for this test case; therefore, all three planet mesh results are identical and only the results for one planet are shown. Comparison of the flexible and nonflexible load plots indicated that while the maximum loads increased, the minimum loads remained nearly the same. There was a similar effect observed in the other plotted parameters; that is, the curves maintained the same general shape, the minimum points did not noticably change, but the maximums increased with the addition of the flexible carrier.

Another test case, Example 4.2, Table 1, was executed for a lightly loaded planetary system with unequal phasing and with a carrier stiffness of 3,000,000 lbs/in and a pin stiffness of 5,000,000 lbs/in. The results for this case, Figure 12c, show very little variation from the rigid carrier results, less than 2 %. This variation is most likely due to the very small loads.

It should be noted that this solution consumes considerably more CPU time than a simple planetary or star system due to the larger system of dynamic equations and particularly the increased number of boundary conditions that must converge. It is recommended that the nonflexible solution be run first and the converged boundary conditions be used in conjunction with the output torque term to estimate the new boundary conditions, see Appendix A for details.

Due to funding limitations, a flexible ring rim case was not executed to completion. It has been coded and a test of the first few boundary condition iterations indicated that there should be no significant problems with this code.

VII. CONCLUDING REMARKS

A number of new options have been added to the multiple mesh gear program, but only a few test cases were run for each of these due to the minimum amount of epicyclic data available for comparision. It is recommended that the program be more thoroughly tested and evaluated via parametric studies as well as comparison to test data. Follow on work should also include refinement of the finite element stress sensitivity postprocessing.

A floating sun gear option was added which will allow the user to investigate the effects of various spring rates and damping at the sun center. Several test cases were executed and the program gives reasonable results, with the solution approaching the rigid mount solution as the spring rates become 10 to 15 times the tooth pair stiffnesses.

The critical speeds predicted by the new natural frequency option, and the critical speeds indicted by running speed surveys with the dynamic response solution agreed well with the frequencies for tooth pair stiffnesses at the pitch diameter.

The refined helical gear option lays the foundation for an alternative method of analyzing helical gear dynamics. Due to funding limitations, the potential for the finite element solution was not fully accomplished. However, the finite element results were used to generate a general tooth pair compliance similar to the original spur gear compliance formulation. The stress postprocessing uses the spur gear stress postprocesser which inherently assumes the load line is parallel to the axis of rotation. Thus, the stress postprocessing could have significant errors for large helix angles.

The flexible carrier and flexible ring gear rim options modified the output torque for each segment to vary with the dynamic results while the total output torque remains constant. The test case results were reasonable, with the maximum loads increasing and the minimum loads remaining nearly the same when compared to the rigid carrier results.

VIII. REFERENCES

1. Linda S. Boyd and James Pike, "Multi-Mesh Gear Dynamics Program Evaluation and Enhancements," NASA CR-174747, September 1984.

2. James Pike, "Interactive Multiple Spur Gear Mesh Dynamic Load Program," NASA CR-165514, December, 1981.

3. James Pike, "Expansion of the Dynamic Load Solution for Multiple Planet Spur Gearing to Helical Gearing," Documentation Report to NASA Lewis , September 1983.

4. R. W. Cornell, "Compliance and Stress Sensitivity of Spur Gear Teeth," Journal of Mechanical Design, April 1981, Vol.103.

5. R. W. Cornell, and W. W. Westervelt, "Dynamic Tooth Loads and Stressing for High Contact Ratio Spur Gears", Journal of Mechanical Design, Jan. 1978.

6. H. H. Richardson, "Static and Dynamic Load, Stresses, and Deflection Cycles in Spur-Gear Systems", Sc.D. Thesis; MIT Report, 1958.

7. Teruaki Hidaka, Yoshio Terauchi, and Keiji Dohi "On the Relation between the Run-Out Errors and the Motion of the Center of Sun Gear in a Stoeckicht Planetary Gear," Bulletin of the JSME, vol.22, No. 167, May 1979.

8. J. N. Reddy, An Introduction to the Finite Element Method, McGraw-Hill Book Co., 1984.

9. J. M. Boyle, J. J. Dongarra, B. S. Garbow, and C. B. Moler, Matrix Eigensystem Routines. Eispack Guide Extension. SpringerVerlag, 1977.

IX. BIBLIOGRAPHY

Botman, M.,"Epicyclic Gear Vibrations," Journal of Engineering for Industry, August 1976.

Boyd, Linda S. and Pike, James, "Multi-Mesh Gear Dynamics Program Evaluation and Enhancements," NASA CR-174747, September 1984.

Boyle, J. M., Dongarra, J. J., Garbow, B. S., and Moler C. B., Matrix Eigensystem Routines. Eispack Guide Extension. SpringerVerlag, 1977.

Cornell, R.W., "Compliance and Stress Sensitivity of Spur Gear Teeth," Journal of Mechanical Design, April 1981, Vol.103.

Cornell, R.W., and Westervelt, W. W., "Dynamic Tooth Loads and Stressing for High Contact Ratio Spur Gears", Journal of Mechanical Design, Jan. 1978.

Hidaka, Teruaki, Terauchi, Yoshio, and Dohi, Keiji "On the Relation between the Run-Out Errors and the Motion of the Center of Sun Gear in a Stoeckicht Planetary Gear," Bulletin of the JSME, vol.22, No. 167, May 1979.

Hidaka, Teruaki, Terauchi, Yoshio, and Fujii, Makoto, "Analysis of Dynamic Tooth Load on Planetary Gear," Bulletin of the JSME, Vol. 23, No. 176, February 1980.

Hidaka, Teruaki, Terauchi, Yoshio, Nohara, Minoru, and Oshita, Dynamic Behavior of Planetary Gear (3rd Report, Displacement of Ring Gear in Direction of Line of Action)," Bulletin of the JSME, Vol. 20, No. 150, December 1977.

Pike, James, "Expansion of the Dynamic Load Solution for Multiple Planet Spur Gearing to Helical Gearing," Documentation Report to NASA Lewis , September 1983.

Pike, James, "Interactive Multiple Spur Gear Mesh Dynamic Load Program," NASA CR-165514, December, 1981.

Reddy, J.N., An Introduction to the Finite Element Method, McGraw-Hill Book Co., 1984.

Richardson, H.H., "Static and Dynamic Load, Stresses, and Deflection Cycles in Spur-Gear Systems", Sc.D. Thesis; MIT Report, 1958.

X. TABLES

TABLE 1: DESCRIPTION OF TEST CASES

Example Case	Number Of Planets	Diametral Pitch	Pressure Angle	Number of Teeth			Face Width			Helix Angle
				Sun	Planet	Ring	Sun (in.)	Planet (in.)	Ring (in.)	
TASK 1 - Floating Sun										
Example 1.1	3	8.4667	22.5	14	28	70	1.18	1.18	1.42	0
TASK 2 - Natural Frequency										
Example 2.1	2	11.01	25	24	77	-	2.22	1.90	-	0
Example 2.2	3	19.2	22.5	27	45	117	1.222	1.222	0.945	0
TASK 3 - Refined Helical Compliance										
Example 3.1	2	7.167	22.5	39	46	131	2.70	2.41	2.75	12.383
TASK 4 - Flexible Carrier Evaluation										
Example 4.1	3	19.2	22.5	27	45	117	1.222	1.222	0.945	0
Example 4.2	3	8.4667	22.5	14	28	70	1.18	1.18	1.42	0

TABLE 2: FLOATING SUN TEST CASE RESULTS

Planet Number	K_x (lb/in)	K_y (lb/in)	D_x (lb-s/in)	D_y (lb-s/in)	Maximum Load		Percent Difference From Non Flexible Maximum Load	
					Sun-Planet	Ring-Planet	Sun-Planet	Ring-Planet
1	-	-	-	-	19.13	17.05		
2	-	-	-	-	19.19	15.85		
3	-	-	-	-	19.32	16.03		
1	10×10^6	10×10^6	.05	.05	20.42	19.44	6.7	14.0
2					20.34	18.08	6.0	14.1
3					19.68	18.47	1.9	15.2
1	30×10^6	30×10^6	.02	.02	19.26	17.77	0.68	4.2
2					19.72	16.57	2.8	4.5
3					19.64	16.95	1.7	5.7

XI. FIGURES

Figure 1. Floating Sun Model

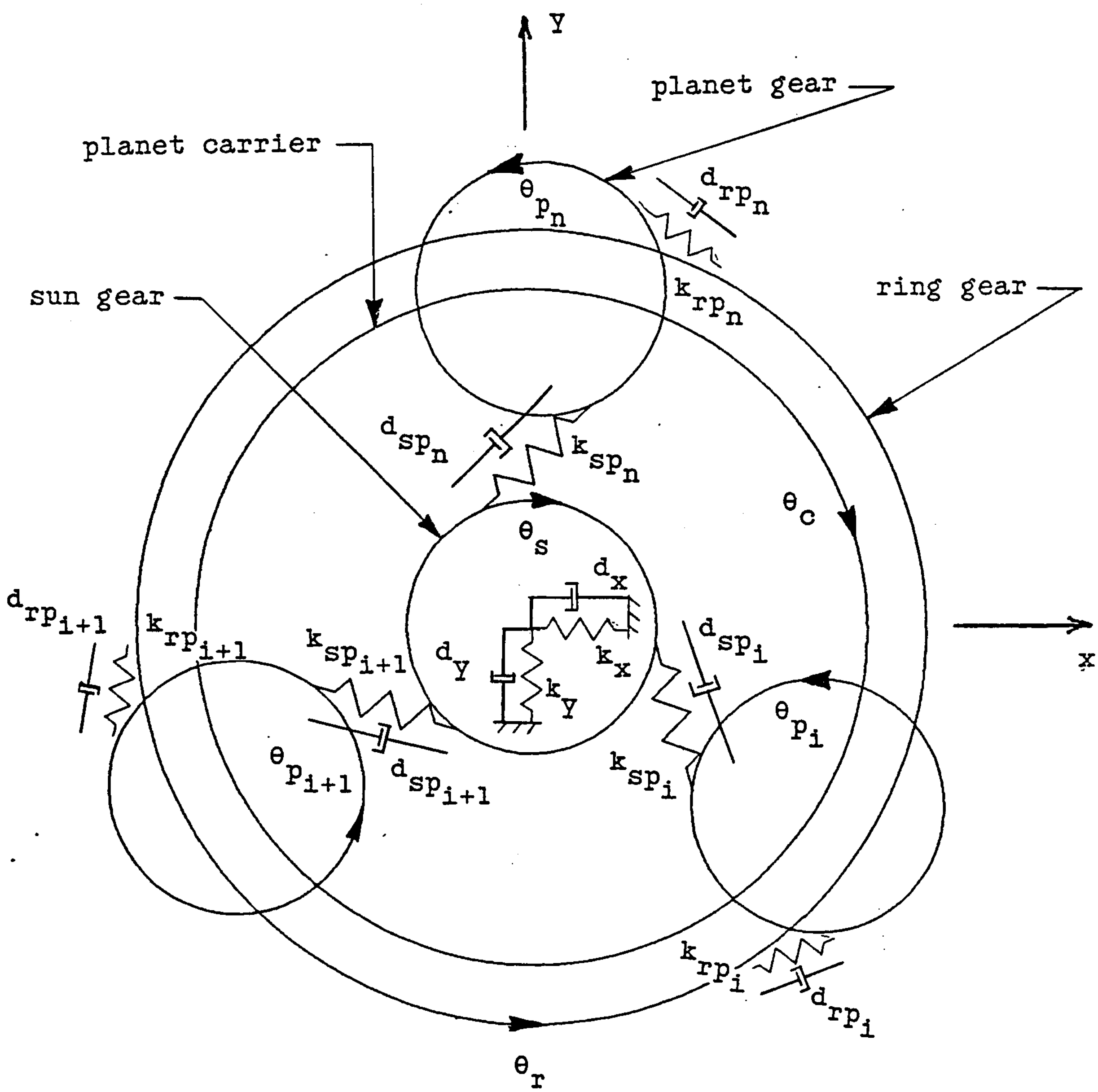

Figure 2. Flowchart for Natural Frequency Modifications

Subroutine FREQ is called from READ2

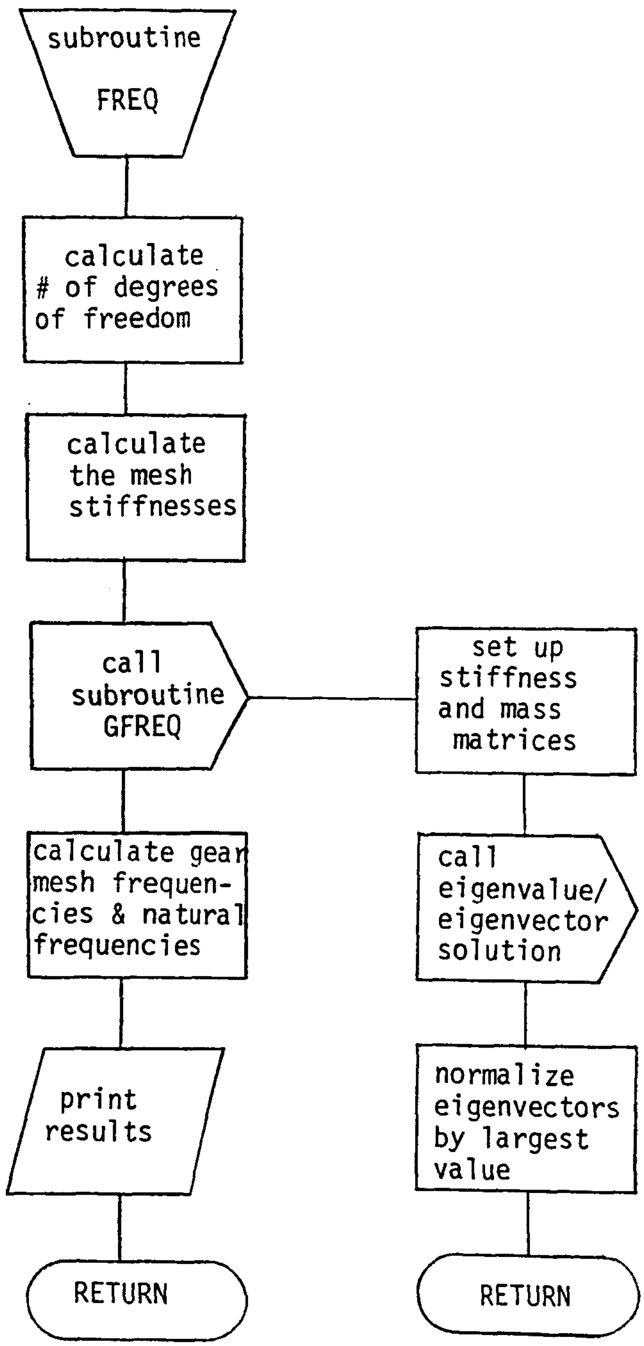

Figure 3. Natural Frequency Interference Plots, Example 1

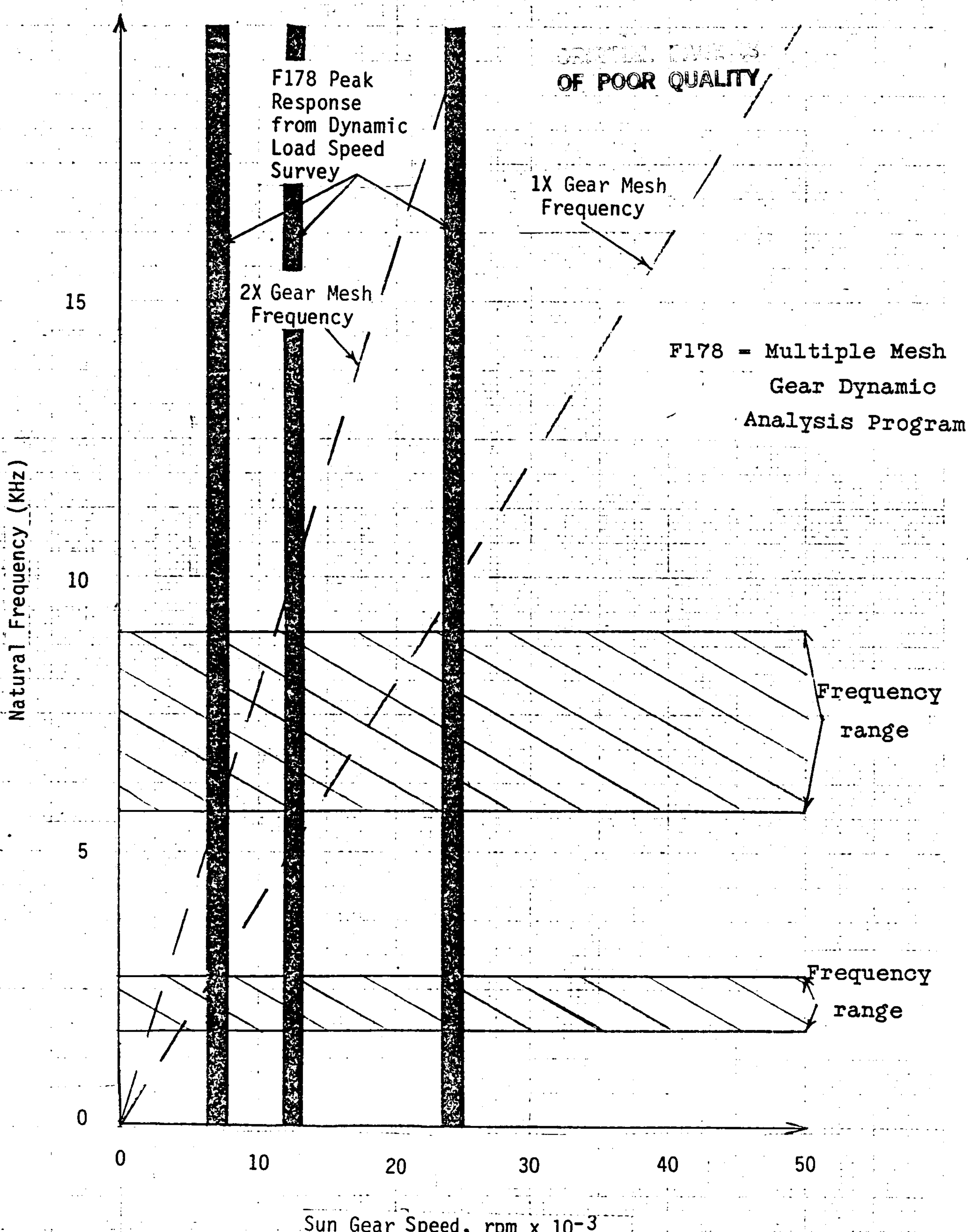

Figure 4. Natural Frequency Interference Plots, Example 2

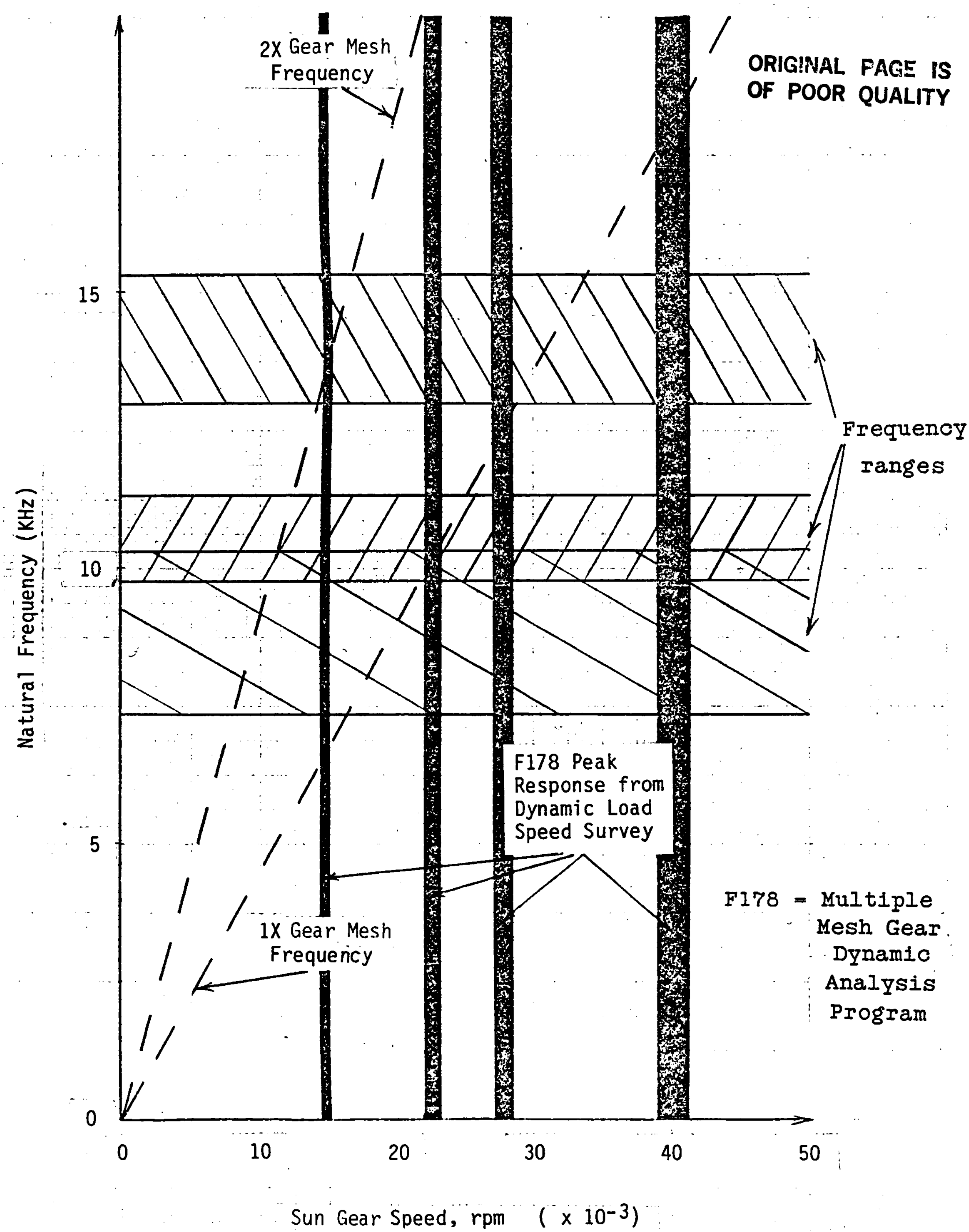

Figure 5. Natural Frequency vs. Percent Mesh Time

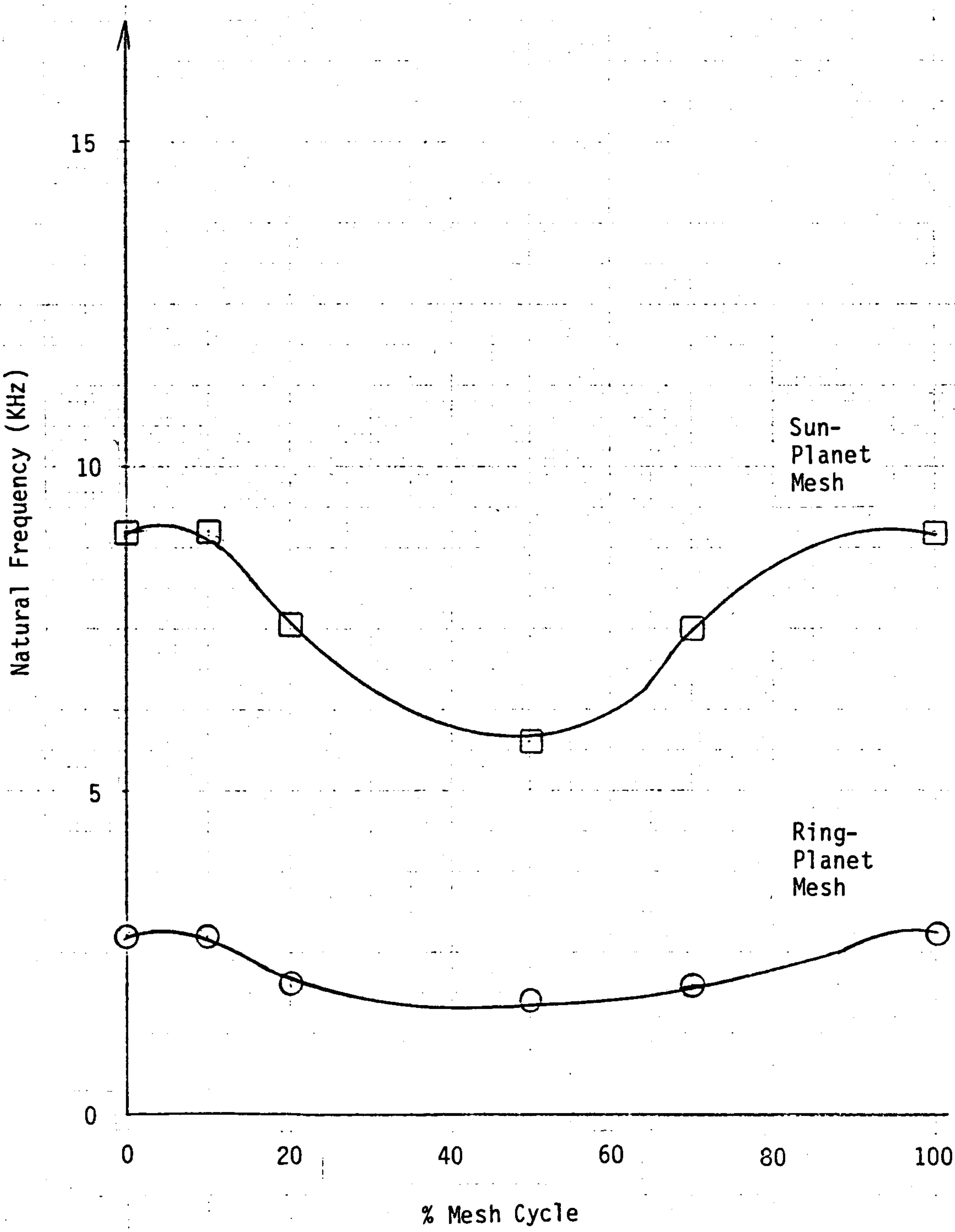

(for instantaneous stiffness)

Figure 6. Flowchart for Helical Tooth Compliance Modifications

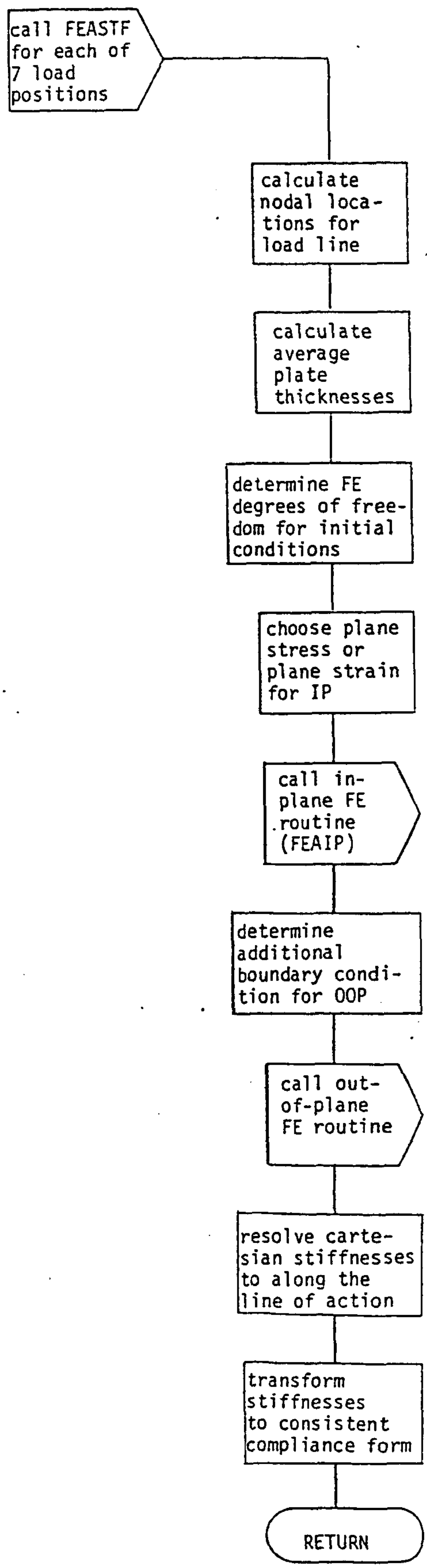

ORIGINAL PAGE IS OF POOR QUALITY

Abbreviations

FE = Finite Element
IP = In-Plane
OOP = Out-of-Plane

Figure 7. Helical Gear Tooth Finite Element Model

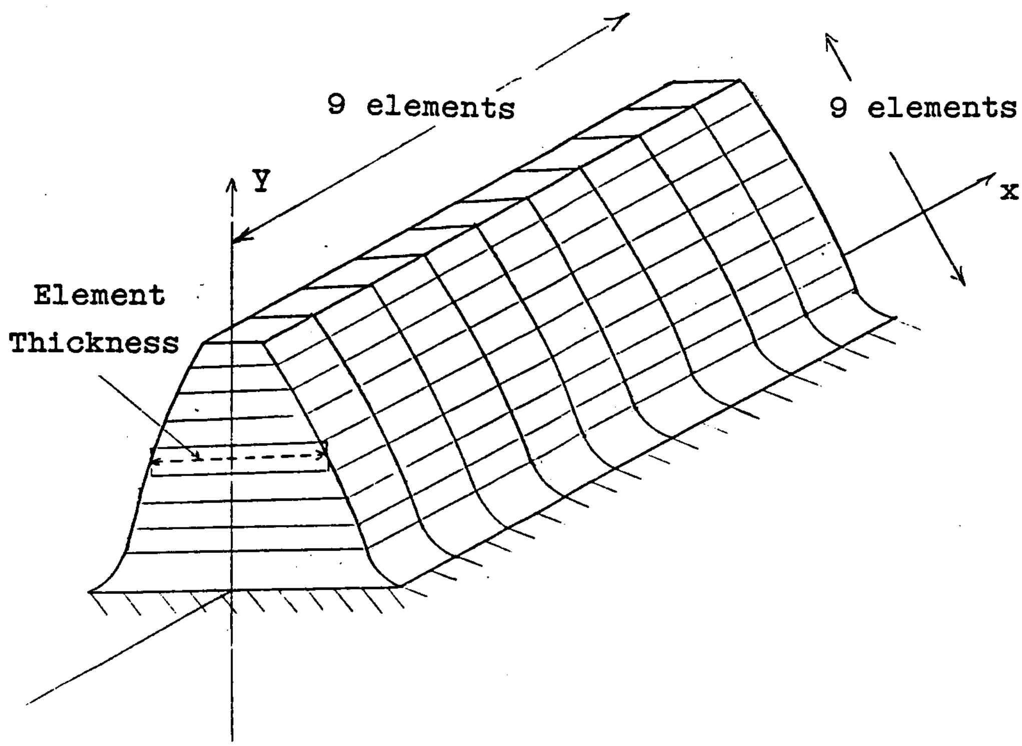

Figure 8. Program Output from Finite Element Helical Gear Option

F 1 7 8

PROGRAM FEATURES OF THE 1985 VERSION

1. CALCULATES DYNAMIC LOAD RESPONSE FOR
   A. SINGLE MESH SPUR GEARING
   B. MULTIPLE MESH SPUR GEARING, STAR OR PLANETARY
   C. SINGLE MESH HELICAL GEARING
   D. MULTIPLE MESH HELICAL GEARING
   E. DOUBLE HELICAL GEARING
   F. THE CARRIER OR GEAR RIM FLEXIBILITIES ALONG THE RESPECTIVE LINES-OF-ACTION CAN BE ACCOUNTED FOR IN THE DYNAMIC LOAD SOLUTION
   G. A FLOATING SUN GEAR CAN BE INCLUDED IN THE DYNAMIC SOLUTION FOR MULTIPLE MESH SPUR GEARS

2. GEOMETRIC PREPROCESSOR CAN BE USED FOR
   A. INVOLUTE SPUR AND HELICAL TOOTH FORMS
   B. INVOLUTE BUTTRESSED TOOTH FORMS
   C. EXTERNAL AND INTERNAL TOOTH FORMS
   D. MEASUREMENT OVER WIRES DATA
   E. TOLERANCE AND INTERFERENCE CHECKING
   F. INVOLUTE MODIFICATION TABLES

3. STRESS POSTPROCESSOR CAN BE USED FOR
   A. DYNAMIC LOAD SUMMARY
   B. MODIFIED HEYWOOD STRESS SENSITIVITY
   C. HERTZ STRESSING
   D. FLASH TEMPERATURE SUMMARY
   E. PRESSURE-SLIDING VELOCITY(PV) SUMMARY

4. DYNAMIC LOAD SOLUTION ASSUMPTIONS
   A. CIRCUMFERENTIALLY STIFF RING GEAR
   B. CIRCUMFERENTIALLY STIFF PLANET CARRIER
   C. EQUILIBRIUM EQUATIONS DO NOT INCLUDE FRICTION
   D. INPUT TORQUE IS CONSTANT

5. GEOMETRIC DATA IN ROTATIONAL PLANE UNLESS NOTED
   A. ANGLES ARE IN DEGREES
   B. FORCES ARE IN POUNDS(#)
   C. LENGTHS ARE IN INCHES(IN)
   D. MASSES ARE IN (#-SEC**2/IN)
   E. STRESSES ARE IN PSI(#/IN**2)
   F. TEMPERATURES ARE IN DEGREES FAHRENHEIT

THIS PROGRAM WAS DEVELOPED AT HAMILTON STANDARD DIVISION OF UNITED TECHNOLOGIES , WINDSOR LOCKS , CONN. BY J. PIKE, R. CORNELL, W. WESTERVELT, AND L. BOYD. FUNDING WAS GIVEN UNDER CONTRACT BY NASA-LEWIS , CLEVELAND AND MONITORED BY D. TOWNSEND.

ORIGINAL PAGE IS
OF POOR QUALITY

Figure 8 (cont)

SUN-PLANET MESH

ROTATIONAL PLANE
INVOLUTE MODIFICATIONS
****

(ENGAGEMENT)

PINION LOC.	INV. MODIFIC. MIN.	MAX.	DIA.	ROLL ANG.	GEAR INV. MODIFIC. MIN.	MAX.	DIA.	ROLL ANG.
0.0	0.000000	0.000000	5.4042	18.3253	0.000000	0.000000	6.7722	28.3170
0.1	0.000004	0.000004	5.3993	18.1451	0.000006	0.000006	6.7794	28.4697
0.2	0.000016	0.000016	5.3944	17.9648	0.000024	0.000024	6.7866	28.6226
0.3	0.000036	0.000036	5.3896	17.7847	0.000054	0.000054	6.7939	28.7754
0.4	0.000064	0.000064	5.3848	17.6044	0.000096	0.000096	6.8011	28.9282
0.5	0.000100	0.000100	5.3801	17.4241	0.000150	0.000150	6.8085	29.0810
0.6	0.000144	0.000144	5.3754	17.2439	0.000216	0.000216	6.8158	29.2338
0.7	0.000196	0.000196	5.3707	17.0636	0.000294	0.000294	6.8232	29.3866
0.8	0.000256	0.000256	5.3661	16.8834	0.000384	0.000384	6.8306	29.5395
0.9	0.000324	0.000324	5.3616	16.7031	0.000486	0.000486	6.8380	29.6923
1.0	0.000400	0.000400	5.3571	16.5230	0.000600	0.000600	6.8455	29.8450

(DISENGAGEMENT)

PINION LOC.	INV. MODIFIC. MIN.	MAX.	DIA.	ROLL ANG.	GEAR INV. MODIFIC. MIN.	MAX.	DIA.	ROLL ANG.
0.0	0.000000	0.000000	5.7787	29.2367	0.000000	0.000000	6.3985	19.06611
0.1	0.000000	0.000000	5.7862	29.4200	0.000010	0.000010	6.3933	18.91061
0.2	0.000000	0.000000	5.7938	29.6036	0.000040	0.000040	6.3882	18.75501
0.3	0.000000	0.000000	5.8014	29.7870	0.000090	0.000090	6.3831	18.59951
0.4	0.000000	0.000000	5.8090	29.9704	0.000160	0.000160	6.3780	18.44391
0.5	0.000000	0.000000	5.8166	30.1540	0.000250	0.000250	6.3730	18.28841
0.6	0.000000	0.000000	5.8243	30.3374	0.000360	0.000360	6.3680	18.13291
0.7	0.000000	0.000000	5.8321	30.5209	0.000490	0.000490	6.3630	17.97721
0.8	0.000000	0.000000	5.8398	30.7043	0.000640	0.000640	6.3581	17.82171
0.9	0.000000	0.000000	5.8476	30.8878	0.000810	0.000810	6.3532	17.66611
1.0	0.000000	0.000000	5.8555	31.0713	0.001000	0.001000	6.3484	17.51071

Figure 8 (cont)

HELICAL GEAR DATA FOR SUN-PLANET MESH

HELIX ANGLE	(DEGREES)	12.383
LEAD OF SUN GEAR	(INCHES)	79.722
LEAD OF PLANET GEAR	(INCHES)	94.031
LOAD LINE INCLINATION	(DEGREES)	0.078
FACE CONTACT RATIO		1.037
INVOLUTE CONTACT RATIO		1.576
TOTAL CONTACT RATIO		2.613
ACTIVE FACE WIDTH		2.120
CROWNED EDGE RELIEF OF ENGAGE		0.0001
CROWNED EDGE RELIEF OF DISENG		0.0001
CROWNED FACE LENGTH OF ENGAGE		0.500
CROWNED FACE LENGTH OF DISENG		0.500
HELIX PHASING CONSTANT		1.03711

Figure 8 (cont)

RING-PLANET MESH

ROTATIONAL PLANE
INVOLUTE MODIFICATIONS
****

(ENGAGEMENT)

	PINION				GEAR			
LOC.	INV. MODIFIC. MIN.	INV. MODIFIC. MAX.	DIA.	ROLL ANG.	INV. MODIFIC. MIN.	INV. MODIFIC. MAX.	DIA.	ROLL ANG.
0.0	0.000000	0.000200	6.4348	20.1246	0.000000	0.000200	18.5713	22.4656
0.1	0.000009	0.000207	6.4222	19.7638	0.000006	0.000204	18.5574	22.3389
0.2	0.000036	0.000228	6.4099	19.4029	0.000024	0.000216	18.5435	22.2122
0.3	0.000081	0.000263	6.3977	19.0422	0.000054	0.000236	18.5297	22.0856
0.4	0.000144	0.000312	6.3858	18.6813	0.000096	0.000264	18.5160	21.9590
0.5	0.000225	0.000375	6.3740	18.3205	0.000150	0.000300	18.5024	21.8321
0.6	0.000324	0.000452	6.3625	17.9597	0.000216	0.000344	18.4888	21.7055
0.7	0.000441	0.000543	6.3511	17.5988	0.000294	0.000396	18.4753	21.5788
0.8	0.000576	0.000648	6.3400	17.2382	0.000384	0.000456	18.4618	21.4520
0.9	0.000729	0.000767	6.3291	16.8774	0.000486	0.000524	18.4485	21.3255
1.0	0.000900	0.000900	6.3184	16.5165	0.000600	0.000600	18.4352	21.1987

(DISENGAGEMENT)

	PINION				GEAR			
LOC.	INV. MODIFIC. MIN.	INV. MODIFIC. MAX.	DIA.	ROLL ANG.	INV. MODIFIC. MIN.	INV. MODIFIC. MAX.	DIA.	ROLL ANG.
0.0	0.000000	0.000200	6.7043	26.8398	0.000000	0.000200	18.8427	24.82381
0.1	0.000000	0.000198	6.7184	27.1506	0.000015	0.000213	18.8558	24.93271
0.2	0.000000	0.000192	6.7325	27.4612	0.000060	0.000252	18.8690	25.04191
0.3	0.000000	0.000182	6.7468	27.7720	0.000135	0.000317	18.8822	25.15101
0.4	0.000000	0.000168	6.7612	28.0828	0.000240	0.000408	18.8954	25.26011
0.5	0.000000	0.000150	6.7758	28.3935	0.000375	0.000525	18.9087	25.36921
0.6	0.000000	0.000128	6.7905	28.7042	0.000540	0.000668	18.9221	25.47831
0.7	0.000000	0.000102	6.8053	29.0149	0.000735	0.000837	18.9355	25.58751
0.8	0.000000	0.000072	6.8202	29.3257	0.000960	0.001032	18.9489	25.69651
0.9	0.000000	0.000038	6.8353	29.6364	0.001215	0.001253	18.9624	25.80571
1.0	0.000000	0.000000	6.8505	29.9471	0.001500	0.001500	18.9760	25.91481

Figure 8 (cont)

INPUT DATA

NO.TEETH - PLANET(EXTERNAL GEAR)	46.0000
NO.TEETH - RING (INTERNAL GEAR)	131.0000
PRESSURE ANGLE (DEGREES) DRIVE SIDE	22.5000
DIAMETRAL PITCH	7.1667
TOOTH TIP RADIUS TOL. (INCH)	0.0020
EDGE BREAK ON TOPLAND (INCH)	0.0100
MACHINED BACKLASH TOL.(INCH)	0.0020
ROOT RADIUS TOL. (INCH)	0.0050
FACE WIDTH - PLANET (INCH)	2.1200
FACE WIDTH - RING (INCH)	2.0700
YOUNGS MOD.*E-6 - PLANET (LB/SQ.INCH)	30.0000
YOUNGS MOD.*E-6 - RING (LB/SQ.INCH)	30.0000
POISSONS RATIO - PLANET	0.3000
POISSONS RATIO - RING	0.3000
SURFACE ROUGHNESS-MAX (AA)	125.0000
OIL INLET TEMPERATURE (DEG.F)	180.0000
INITIAL RPM OF RANGE	10000.0000
FINAL RPM OF RANGE	10000.0000
NUMBER OF INTERVALS	1.0000
TORQUE INPUT (IN-LBS)	76155.0000
TOTAL INV.PROFILE MODIFICATION,ENGAGE (INCH)	0.0015
TOTAL INV.PROFILE MODIFICATION,DISENG (INCH)	0.0015
INV.PROFILE MOD.LOCATION-% OF SOE	50.0000
INV.PROFILE MOD.LOCATION-% OF SOD	50.0000
INV.PROFILE MOD.TOTAL TOLERANCE	0.0000
+C.D.TOL. (OUT OF MESH) (INCH)	0.0000
-C.D.TOL. (INTO MESH) (INCH)	0.0000
CONTACT RATIO INPUT	1.0000
HERTZ CONSTANT FOR COMPLIANCE	261402.
CENTER DISTANCE,THEO. (INCH)	6.0714
CENTER DISTANCE,MAX. (INCH)	6.0714
CENTER DISTANCE,MIN. (INCH)	6.0714
CIRCULAR PITCH (INCH)	0.4488
CIRCULAR BASE PITCH (INCH)	0.4146
MAX.OPERATING PRESS. ANGLE (DEG) DRIVE	22.5000
MIN.OPERATING PRESS. ANGLE (DEG) DRIVE	22.5000
NOMINAL CONTACT RATIO AT C.D.-THEO.	1.7161
MINIMUM CONTACT RATIO AT C.D.-MAX.	1.5702
MATERIAL CONSTANT	0.0528
CODE FOR TYPE OF OIL	0.0000

		PLANET	RING
NUMBER OF TEETH		46.0000	131.0000
PITCH DIAMETER	(INCH)	6.5714	18.7142
BASE CIRCLE DIA. DRIVE SIDE	(INCH)	6.0712	17.2897
TOOTH TIP DIAMETER,MAX.	(INCH)	6.8505	18.4392
TOOTH TIP DIAMETER,MIN.	(INCH)	6.8465	18.4352
EFFECTIVE TOOTH TIP DIA	(INCH)	6.8265	18.4592
ROOT DIAMETER,MAX.	(INCH)	6.2246	19.0469
ROOT DIAMETER,MIN.	(INCH)	6.2146	19.0369
TRUE INV.FORM DIA.	(INCH)	6.3184	18.9760
TOPLAND WIDTH,MIN.	(INCH)	0.1036	0.1157
ROOT FILLET RADIUS,MIN.	(INCH)	0.0599	0.0553
MACHINE BACKLASH,MAX.	(INCH)	0.0025	0.0025
MACHINE BACKLASH,MIN.	(INCH)	0.0005	0.0005
CIRCULAR TOOTH THICKNESS	(INCH)	0.2297	0.2297
MACH.CIRC.TOOTH THKNS.MAX.	(INCH)	0.2297	0.2297
MACH.CIRC.TOOTH THKNS.MIN.	(INCH)	0.2277	0.2277
TIP/ROOT CLEAR.MIN AT CD MIN.	(INCH)	0.0339	0.0218
ROLL ANGLE AT TOOTH TIP DIA.	(DEG)	29.9470	21.1987
ROLL ANGLE	(DEG)	26.8398	24.9994
AT ADD.INV.MODIFICATION DIA.	(INCH)	6.7043	18.8638
ROLL ANGLE AT PITCH DIA.	(DEG)	23.7326	23.7326
ROLL ANGLE	(DEG)	20.1246	22.6414
AT DED.INV.MODIFICATION DIA.	(INCH)	6.4348	18.5907
ROLL ANGLE AT TIFD	(DEG)	16.5164	25.9148
INSPECTION WIRE/BALL DIA.	(INCH)	0.2450	0.2400
MAX.MEASUREMENT OVER 2 WIRE/BALL	(INCH)	6.9370	18.3576
MIN.MEASUREMENT OVER 2 WIRE/BALL	(INCH)	6.9325	18.3626
EFFECTIVE WIDTH AT TOOTH TIP		2.1200	2.0700
EFFECTIVE WIDTH AT START OF FILLET		2.1200	2.0700
RADIUS TO BASE OF FILLET INPUT	(INCH)	0.0000	0.0000
OUTSIDE RADIUS INPUT	(INCH)	0.0000	0.0000
FILLET RADIUS INPUT	(INCH)	0.0000	0.0000
DAMPING RATIO INPUT		0.2000	0.2000

Figure 8 (cont)

```
HELICAL GEAR DATA FOR RING-PLANET MESH

HELIX ANGLE             (DEGREES)        12.383
LEAD OF PLANET GEAR     (INCHES)         94.031
LEAD OF RING GEAR       (INCHES)        267.783
LOAD LINE INCLINATION   (DEGREES)         0.078
FACE CONTACT RATIO                        1.013
INVOLUTE CONTACT RATIO                    1.716
TOTAL CONTACT RATIO                       2.729
ACTIVE FACE WIDTH                         2.070
CROWNED EDGE RELIEF OF ENGAGE             0.0001
CROWNED EDGE RELIEF OF DISENG             0.0001
CROWNED FACE WIDTH OF ENGAGE              0.300
CROWNED FACE WIDTH OF DISENG              0.300
HELIX ANGLE PHASING CONSTANT              1.01265


NUMBER OF PLANETS                                  2
NUMBER OF BOUNDARY CONDITION ITERATIONS           10
TOLERANCE FOR BOUNDARY CONDITION CONVERGENCE  0.10000E+00

EQUIVALENT MASS OF SUN GEAR                  0.18800E-01
EQUIVALENT MASS OF PLANET CARRIER            0.97400E-01
EQUIVALENT MASS OF RING GEAR                 0.00000E+00
EQUIVALENT MASS OF PLANET # 1                0.21600E-01

          C O M P L I A N C E   C O N S T A N T S

SUN-PLANET

0.1583E-06 * ( 1 + -0.8254E-01 * (S/SO) +  0.8360E+00 * (S/SO)**2 +  0.4108E-01 * (S/SO)**3 + -0.2646E+00 * (S/SO)**4 )

RING-PLANET

0.1730E-06 * ( 1 +  0.5929E-01 * (S/SO) +  0.6488E+00 * (S/SO)**2 + -0.1420E+00 * (S/SO)**3 + -0.2578E+00 * (S/SO)**4 )

             ************* PLANETARY GEAR SYSTEM ************
```

B O U N D A R Y   C O N D I T I O N   I T E R A T I O N   R E S U L T S   Figure 8 (cont)

```
SUN-PLANET;  MESHES 1 THRU N, LEFT TO RIGHT
ITERATION, END DISPLACEMENT      2  0.15479E-02  0.18250E-02
STARTING DISPLACEMENT               0.15842E-02  0.16367E-02
ITERATION, ENDING VELOCITY       2  0.21040E+02 -0.26328E+02
STARTING VELOCITY                   0.16157E+02 -0.23516E+02

RING-PLANET;  MESHES 1 THRU N, LEFT TO RIGHT
ITERATION, END DISPLACEMENT      2  0.19363E-02  0.16605E-02
STARTING DISPLACEMENT               0.17082E-02  0.16562E-02
ITERATION, ENDING VELOCITY       2 -0.22162E+02  0.25209E+02
STARTING VELOCITY                  -0.28834E+02  0.10843E+02

SUN-PLANET;  MESHES 1 THRU N, LEFT TO RIGHT
ITERATION, END DISPLACEMENT      3  0.14964E-02  0.18368E-02
STARTING DISPLACEMENT               0.15479E-02  0.18250E-02
ITERATION, ENDING VELOCITY       3  0.21247E+02 -0.26198E+02
STARTING VELOCITY                   0.21040E+02 -0.26328E+02

RING-PLANET;  MESHES 1 THRU N, LEFT TO RIGHT
ITERATION, END DISPLACEMENT      3  0.18681E-02  0.15293E-02
STARTING DISPLACEMENT               0.19363E-02  0.16605E-02
ITERATION, ENDING VELOCITY       3 -0.21635E+02  0.25814E+02
STARTING VELOCITY                  -0.22162E+02  0.25209E+02

PLANET NUMBER   1
RPM =     10000.00

MAXIMUM LOAD FOR SUN-PLANET =     15280.17

MAXIMUM LOAD FOR RING-PLANET =     12795.10

PLANET NUMBER   2
RPM =     10000.00

MAXIMUM LOAD FOR SUN-PLANET =     15287.16

MAXIMUM LOAD FOR RING-PLANET =     12502.19
```

Figure 8 (cont)

NO TOOTH ERRORS SOLUTION

MAXIMUM VALUES FOR SUN-PLANET MESH 1

	SUN		PLANET
FILLET STRESS CONCENTRATION (KSUBT)	1.48134		1.48045
MAXIMUM HERTZ STRESS	255258.7		255258.7
MAXIMUM HERTZ STRESS AT PD	206045.6		206045.6
MAXIMUM BENDING STRESS	107946.4		94838.1
MAXIMUM BENDING STRESS AT PD	55945.5		55044.5
DEPTH TO MAXIMUM SHEAR	0.01406		0.01406
MAXIMUM DYNAMIC PV(MILLIONS OF PSI*FT/MIN)	580.14429		580.14429
MAXIMUM FLASH TEMPERATURE		276.3	
MAXIMUM NORMAL LOAD		15280.2	
AVERAGE COEFFICIENT OF FRICTION		0.08840	
RPM FOR STRESSES		10000.00	

*
THE EFFECTIVE CONTACT RATIO = 1.5800
*

MAXIMUM VALUES FOR SUN-PLANET MESH 2

	SUN		PLANET
FILLET STRESS CONCENTRATION (KSUBT)	1.52691		1.45766
MAXIMUM HERTZ STRESS	255319.1		255319.1
MAXIMUM HERTZ STRESS AT PD	193971.0		193971.0
MAXIMUM BENDING STRESS	108625.4		96478.6
MAXIMUM BENDING STRESS AT PD	74544.4		34543.2
DEPTH TO MAXIMUM SHEAR	0.01406		0.01406
MAXIMUM DYNAMIC PV(MILLIONS OF PSI*FT/MIN)	582.11499		582.11499
MAXIMUM FLASH TEMPERATURE		277.7	
MAXIMUM NORMAL LOAD		15287.2	
AVERAGE COEFFICIENT OF FRICTION		0.02433	
RPM FOR STRESSES		10000.00	

*
THE EFFECTIVE CONTACT RATIO = 1.5800
*

MAXIMUM VALUES FOR RING-PLANET MESH 1

	PLANET		RING
FILLET STRESS CONCENTRATION (KSUBT)	1.52831		1.58517
MAXIMUM HERTZ STRESS	178244.5		178244.5
MAXIMUM HERTZ STRESS AT PD	139438.2		139438.2
MAXIMUM BENDING STRESS	92848.5		75782.4
MAXIMUM BENDING STRESS AT PD	71376.2		21364.0
DEPTH TO MAXIMUM SHEAR	0.01690		0.01690
MAXIMUM DYNAMIC PV(MILLIONS OF PSI*FT/MIN)	157.38115		157.38115
MAXIMUM FLASH TEMPERATURE		208.6	
MAXIMUM NORMAL LOAD		12795.1	
AVERAGE COEFFICIENT OF FRICTION		0.02975	

```
RPM FOR STRESSES                                          10000.00

* * * * * * * * * * * * * * * * * * * *
    THE EFFECTIVE CONTACT RATIO =  1.6100
* * * * * * * * * * * * * * * * * * * *
```

Figure 8 (cont)

```
                    MAXIMUM VALUES FOR RING-PLANET MESH   2

                                                      PLANET                 RING
FILLET STRESS CONCENTRATION (KSUBT)                  1.48045               1.61290
MAXIMUM HERTZ STRESS                               177345.0              177345.0
MAXIMUM HERTZ STRESS AT PD                         159500.1              159500.1
MAXIMUM BENDING STRESS                              87345.4               68110.6
MAXIMUM BENDING STRESS AT PD                        54211.2               44304.4
DEPTH TO MAXIMUM SHEAR                              0.01660               0.01660
MAXIMUM DYNAMIC PV(MILLIONS OF PSI*FT/MIN)        152.18002             152.18002
MAXIMUM FLASH TEMPERATURE                                       206.3
MAXIMUM NORMAL LOAD                                           12502.2
AVERAGE COEFFICIENT OF FRICTION                               0.09525
RPM FOR STRESSES                                             10000.00

* * * * * * * * * * * * * * * * * * * *
    THE EFFECTIVE CONTACT RATIO =  1.6200
* * * * * * * * * * * * * * * * * * * *
```

Figure 9. Fillet Element Thickness

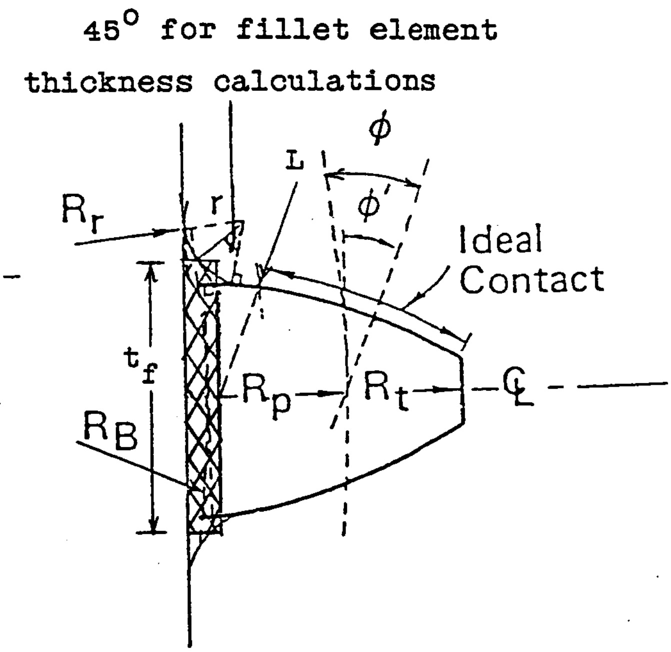

R_r = root radius

R_B = base radius

R_p = pitch radius

R_t = tip radius

r = fillet radius

L = load

ϕ = pressure angle

ϕ' = load line angularity

t_f = fillet element thickness

Figure 10. Flexible Carrier/Ring Gear Rim Model

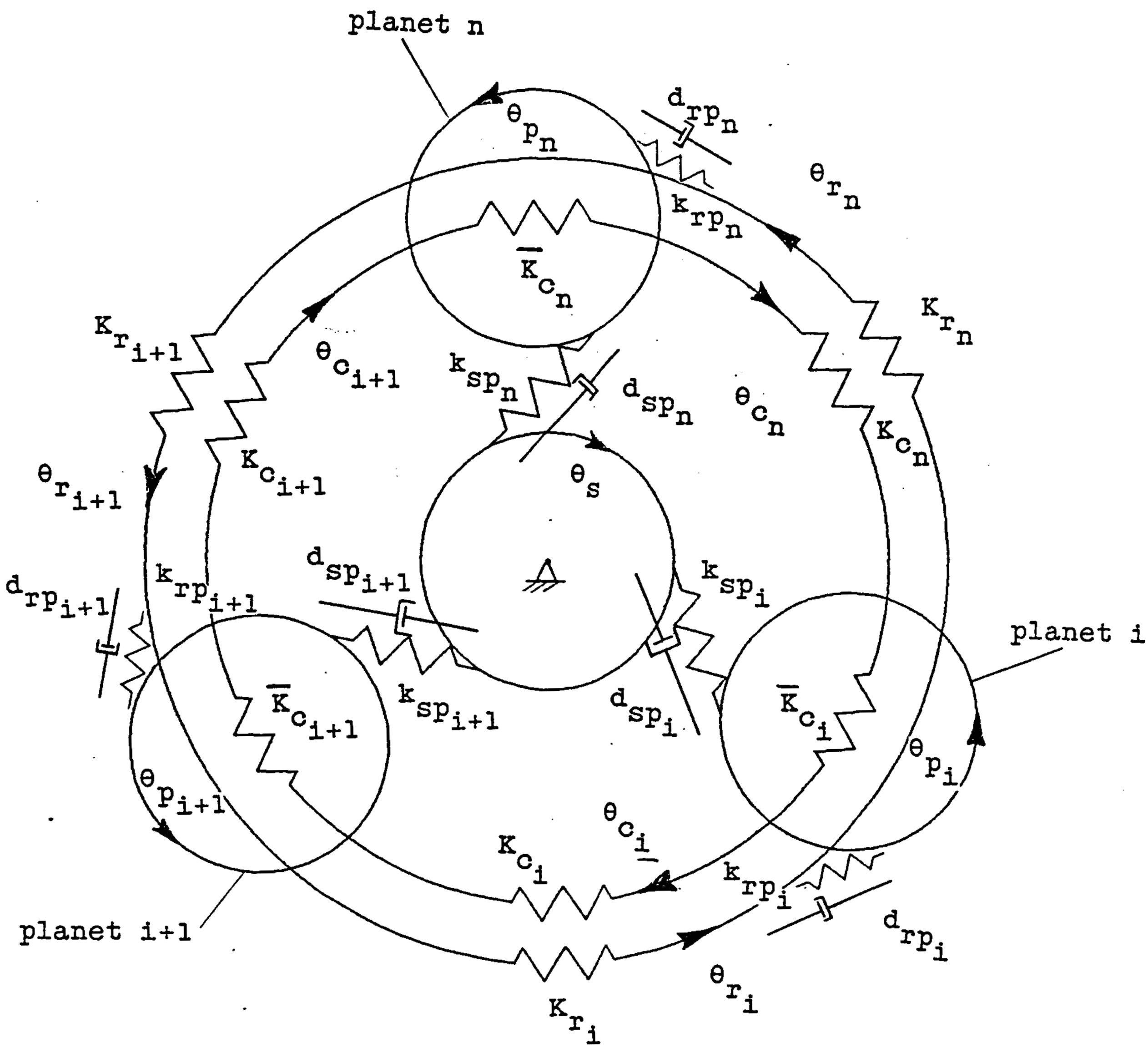

Figure 11. Torque Constraint Model Analogy

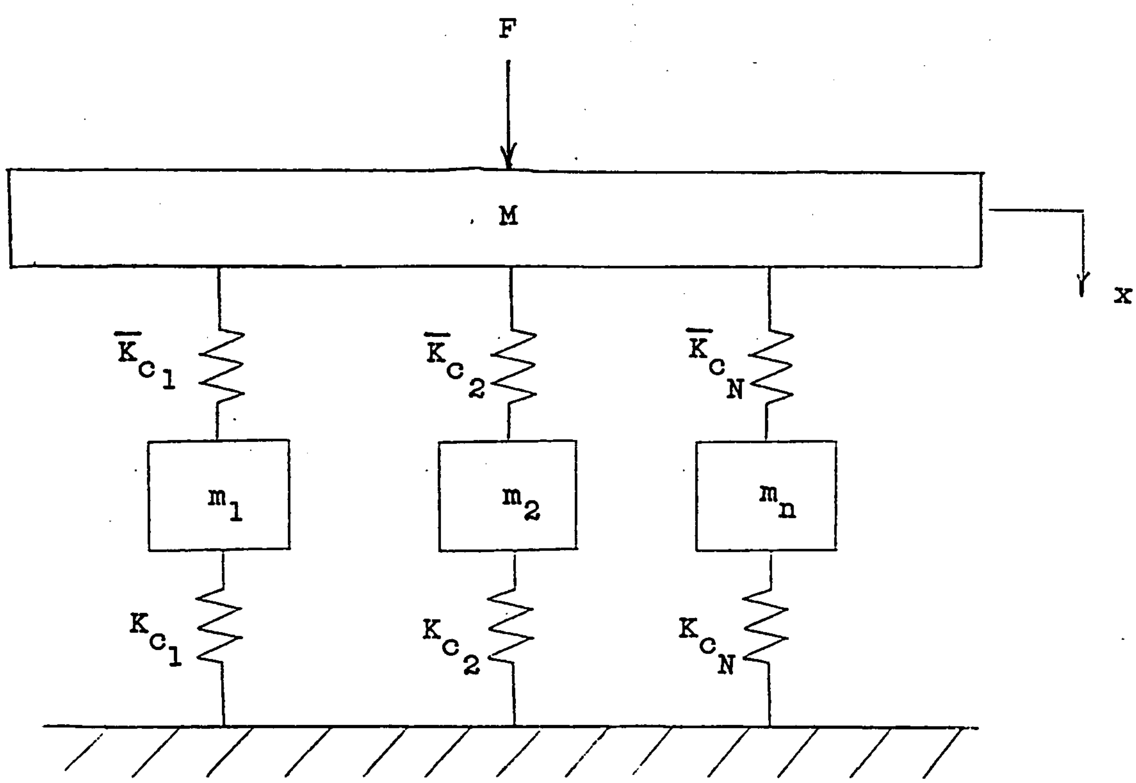

$F = \dfrac{\text{output torque}}{\text{base radius}}$

M = artificial mass

$m_1, m_2, \ldots, m_n$ = planet n effective mass

$\overline{K}_{c_i}$ = carrier pin stiffness

$i = 1, 2, \ldots N$

K_{c_i} = carrier rim segment stiffness

Figure 12a. Flexible Carrier Results, Example 4.1

Flexible Carrier Results

NO TOOTH ERRORS SOLUTION

MAXIMUM VALUES FOR SUN-PLANET MESH 1

	SUN		PLANET
FILLET STRESS CONCENTRATION (KSUBT)	1.58960		1.60189
MAXIMUM HERTZ STRESS	107558.9		107558.9
MAXIMUM HERTZ STRESS AT PD	80165.0		80165.0
MAXIMUM BENDING STRESS	29015.2		19964.9
MAXIMUM BENDING STRESS AT PD	8542.3		10285.5
DEPTH TO MAXIMUM SHEAR	0.00179		0.00179
MAXIMUM DYNAMIC PV(MILLIONS OF PSI*FT/MIN)	396.90015		396.90015
MAXIMUM FLASH TEMPERATURE		199.7	
MAXIMUM NORMAL LOAD		466.3	
AVERAGE COEFFICIENT OF FRICTION		0.07035	
RPM FOR STRESSES		36000.00	
MAXIMUM CARRIER DISPLACEMENT		0.6254E-03	

* * * * * * * * * * * * * * * * * * * *
THE EFFECTIVE CONTACT RATIO = 1.0000
* * * * * * * * * * * * * * * * * * * *

MAXIMUM VALUES FOR SUN-PLANET MESH 2

	SUN		PLANET
FILLET STRESS CONCENTRATION (KSUBT)	1.58960		1.60189
MAXIMUM HERTZ STRESS	107558.9		107558.9
MAXIMUM HERTZ STRESS AT PD	80165.0		80165.0
MAXIMUM BENDING STRESS	29015.2		19964.9
MAXIMUM BENDING STRESS AT PD	8542.3		10285.5
DEPTH TO MAXIMUM SHEAR	0.00179		0.00179
MAXIMUM DYNAMIC PV(MILLIONS OF PSI*FT/MIN)	396.90015		396.90015
MAXIMUM FLASH TEMPERATURE		199.7	
MAXIMUM NORMAL LOAD		466.3	
AVERAGE COEFFICIENT OF FRICTION		0.07035	
RPM FOR STRESSES		36000.00	
MAXIMUM CARRIER DISPLACEMENT		0.6254E-03	

* * * * * * * * * * * * * * * * * * * *
THE EFFECTIVE CONTACT RATIO = 1.0000
* * * * * * * * * * * * * * * * * * * *

MAXIMUM VALUES FOR SUN-PLANET MESH 3

	SUN		PLANET
FILLET STRESS CONCENTRATION (KSUBT)	1.58960		1.60189
MAXIMUM HERTZ STRESS	107558.9		107558.9
MAXIMUM HERTZ STRESS AT PD	80165.0		80165.0
MAXIMUM BENDING STRESS	29015.2		19964.9
MAXIMUM BENDING STRESS AT PD	8542.3		10285.5
DEPTH TO MAXIMUM SHEAR	0.00179		0.00179
MAXIMUM DYNAMIC PV(MILLIONS OF PSI*FT/MIN)	396.90015		396.90015
MAXIMUM FLASH TEMPERATURE		199.7	
MAXIMUM NORMAL LOAD		466.3	
AVERAGE COEFFICIENT OF FRICTION		0.07035	
RPM FOR STRESSES		36000.00	
MAXIMUM CARRIER DISPLACEMENT		0.6254E-03	

* * * * * * * * * * * * * * * * * * * *
THE EFFECTIVE CONTACT RATIO = 1.0000
* * * * * * * * * * * * * * * * * * * *

Non-flexible Carrier Results

NO TOOTH ERRORS SOLUTION

MAXIMUM VALUES FOR SUN-PLANET MESH 1

	SUN		PLANET
FILLET STRESS CONCENTRATION (KSUBT)	1.58960		1.60189
MAXIMUM HERTZ STRESS	104585.0		104585.0
MAXIMUM HERTZ STRESS AT PD	78294.5		78294.5
MAXIMUM BENDING STRESS	27407.3		18876.1
MAXIMUM BENDING STRESS AT PD	8148.3		9811.1
DEPTH TO MAXIMUM SHEAR	0.00174		0.00174
MAXIMUM DYNAMIC PV(MILLIONS OF PSI*FT/MIN)	385.74609		385.74609
MAXIMUM FLASH TEMPERATURE		198.0	
MAXIMUM NORMAL LOAD		440.5	
AVERAGE COEFFICIENT OF FRICTION		0.07019	
RPM FOR STRESSES		36000.00	

* * * * * * * * * * * * * * * * * * * *
THE EFFECTIVE CONTACT RATIO = 1.0000
* * * * * * * * * * * * * * * * * * * *

MAXIMUM VALUES FOR SUN-PLANET MESH 2

	SUN		PLANET
FILLET STRESS CONCENTRATION (KSUBT)	1.58960		1.60189
MAXIMUM HERTZ STRESS	104585.1		104585.1
MAXIMUM HERTZ STRESS AT PD	78294.5		78294.5
MAXIMUM BENDING STRESS	27407.3		18876.2
MAXIMUM BENDING STRESS AT PD	8148.3		9811.1
DEPTH TO MAXIMUM SHEAR	0.00174		0.00174
MAXIMUM DYNAMIC PV(MILLIONS OF PSI*FT/MIN)	385.74634		385.74634
MAXIMUM FLASH TEMPERATURE		198.0	
MAXIMUM NORMAL LOAD		440.5	
AVERAGE COEFFICIENT OF FRICTION		0.07019	
RPM FOR STRESSES		36000.00	

* * * * * * * * * * * * * * * * * * * *
THE EFFECTIVE CONTACT RATIO = 1.0000
* * * * * * * * * * * * * * * * * * * *

MAXIMUM VALUES FOR SUN-PLANET MESH 3

	SUN		PLANET
FILLET STRESS CONCENTRATION (KSUBT)	1.58960		1.60189
MAXIMUM HERTZ STRESS	104584.7		104584.7
MAXIMUM HERTZ STRESS AT PD	78294.4		78294.4
MAXIMUM BENDING STRESS	27407.2		18876.1
MAXIMUM BENDING STRESS AT PD	8148.2		9811.1
DEPTH TO MAXIMUM SHEAR	0.00174		0.00174
MAXIMUM DYNAMIC PV(MILLIONS OF PSI*FT/MIN)	385.74512		385.74512
MAXIMUM FLASH TEMPERATURE		198.0	
MAXIMUM NORMAL LOAD		440.5	
AVERAGE COEFFICIENT OF FRICTION		0.07019	
RPM FOR STRESSES		36000.00	

* * * * * * * * * * * * * * * * * * * *
THE EFFECTIVE CONTACT RATIO = 1.0000
* * * * * * * * * * * * * * * * * * * *

Figure 12a (cont)

Flexible Carrier Results

MAXIMUM VALUES FOR RING-PLANET MESH 1

	PLANET		RING
FILLET STRESS CONCENTRATION (KSUBT)	1.60189		1.96702
MAXIMUM HERTZ STRESS	78270.7		78270.7
MAXIMUM HERTZ STRESS AT PD	65895.3		65895.3
MAXIMUM BENDING STRESS	14193.1		23972.1
MAXIMUM BENDING STRESS AT PD	13575.6		12015.3
DEPTH TO MAXIMUM SHEAR	0.00205		0.00205
MAXIMUM DYNAMIC PV(MILLIONS OF PSI*FT/MIN)	133.13110		133.13110
MAXIMUM FLASH TEMPERATURE		185.5	
MAXIMUM NORMAL LOAD		333.2	
AVERAGE COEFFICIENT OF FRICTION		0.07427	
RPM FOR STRESSES		36000.00	

* * * * * * * * * * * * * * * * * * * *
THE EFFECTIVE CONTACT RATIO = 1.1700
* * * * * * * * * * * * * * * * * * * *

MAXIMUM VALUES FOR RING-PLANET MESH 2

	PLANET		RING
FILLET STRESS CONCENTRATION (KSUBT)	1.60189		1.96702
MAXIMUM HERTZ STRESS	78270.7		78270.7
MAXIMUM HERTZ STRESS AT PD	65895.3		65895.3
MAXIMUM BENDING STRESS	14193.1		23972.1
MAXIMUM BENDING STRESS AT PD	13575.6		12015.3
DEPTH TO MAXIMUM SHEAR	0.00205		0.00205
MAXIMUM DYNAMIC PV(MILLIONS OF PSI*FT/MIN)	133.13110		133.13110
MAXIMUM FLASH TEMPERATURE		185.5	
MAXIMUM NORMAL LOAD		333.2	
AVERAGE COEFFICIENT OF FRICTION		0.07427	
RPM FOR STRESSES		36000.00	

* * * * * * * * * * * * * * * * * * * *
THE EFFECTIVE CONTACT RATIO = 1.1700
* * * * * * * * * * * * * * * * * * * *

MAXIMUM VALUES FOR RING-PLANET MESH 3

	PLANET		RING
FILLET STRESS CONCENTRATION (KSUBT)	1.60189		1.96702
MAXIMUM HERTZ STRESS	78270.7		78270.7
MAXIMUM HERTZ STRESS AT PD	65895.3		65895.3
MAXIMUM BENDING STRESS	14193.1		23972.1
MAXIMUM BENDING STRESS AT PD	13575.6		12015.3
DEPTH TO MAXIMUM SHEAR	0.00205		0.00205
MAXIMUM DYNAMIC PV(MILLIONS OF PSI*FT/MIN)	133.13110		133.13110
MAXIMUM FLASH TEMPERATURE		185.5	
MAXIMUM NORMAL LOAD		333.2	
AVERAGE COEFFICIENT OF FRICTION		0.07427	
RPM FOR STRESSES		36000.00	

* * * * * * * * * * * * * * * * * * * *
THE EFFECTIVE CONTACT RATIO = 1.1700
* * * * * * * * * * * * * * * * * * * *

Non-flexible Carrier Results

MAXIMUM VALUES FOR RING-PLANET MESH 1

	PLANET		RING
FILLET STRESS CONCENTRATION (KSUBT)	1.60189		1.96702
MAXIMUM HERTZ STRESS	73662.1		73662.1
MAXIMUM HERTZ STRESS AT PD	61812.7		61812.7
MAXIMUM BENDING STRESS	12678.2		21217.2
MAXIMUM BENDING STRESS AT PD	11945.5		10572.6
DEPTH TO MAXIMUM SHEAR	0.00194		0.00194
MAXIMUM DYNAMIC PV(MILLIONS OF PSI*FT/MIN)	125.19351		125.19351
MAXIMUM FLASH TEMPERATURE		184.6	
MAXIMUM NORMAL LOAD		296.1	
AVERAGE COEFFICIENT OF FRICTION		0.07371	
RPM FOR STRESSES		36000.00	

* * * * * * * * * * * * * * * * * * * *
THE EFFECTIVE CONTACT RATIO = 1.1700
* * * * * * * * * * * * * * * * * * * *

MAXIMUM VALUES FOR RING-PLANET MESH 2

	PLANET		RING
FILLET STRESS CONCENTRATION (KSUBT)	1.60189		1.96702
MAXIMUM HERTZ STRESS	73662.1		73662.1
MAXIMUM HERTZ STRESS AT PD	61812.8		61812.8
MAXIMUM BENDING STRESS	12678.2		21217.2
MAXIMUM BENDING STRESS AT PD	11945.6		10572.6
DEPTH TO MAXIMUM SHEAR	0.00194		0.00194
MAXIMUM DYNAMIC PV(MILLIONS OF PSI*FT/MIN)	125.19351		125.19351
MAXIMUM FLASH TEMPERATURE		184.6	
MAXIMUM NORMAL LOAD		296.1	
AVERAGE COEFFICIENT OF FRICTION		0.07371	
RPM FOR STRESSES		36000.00	

* * * * * * * * * * * * * * * * * * * *
THE EFFECTIVE CONTACT RATIO = 1.1700
* * * * * * * * * * * * * * * * * * * *

MAXIMUM VALUES FOR RING-PLANET MESH 3

	PLANET		RING
FILLET STRESS CONCENTRATION (KSUBT)	1.60189		1.96702
MAXIMUM HERTZ STRESS	73662.1		73662.1
MAXIMUM HERTZ STRESS AT PD	61812.7		61812.7
MAXIMUM BENDING STRESS	12678.2		21217.2
MAXIMUM BENDING STRESS AT PD	11945.5		10572.6
DEPTH TO MAXIMUM SHEAR	0.00194		0.00194
MAXIMUM DYNAMIC PV(MILLIONS OF PSI*FT/MIN)	125.19341		125.19341
MAXIMUM FLASH TEMPERATURE		184.6	
MAXIMUM NORMAL LOAD		296.1	
AVERAGE COEFFICIENT OF FRICTION		0.07371	
RPM FOR STRESSES		36000.00	

* * * * * * * * * * * * * * * * * * * *
THE EFFECTIVE CONTACT RATIO = 1.1700
* * * * * * * * * * * * * * * * * * * *

Figure 12b. Flexible Carrier Results, Example 4.2

Flexible Carrier Results

MAXIMUM VALUES FOR SUN-PLANET MESH 1

	SUN		PLANET
FILLET STRESS CONCENTRATION (KSUBT)	1.43617		1.39553
MAXIMUM HERTZ STRESS	19740.2		19740.2
MAXIMUM HERTZ STRESS AT PD	19412.7		19412.7
MAXIMUM BENDING STRESS	276.8		301.0
MAXIMUM BENDING STRESS AT PD	257.3		293.5
DEPTH TO MAXIMUM SHEAR	0.00041		0.00041
MAXIMUM DYNAMIC PV(MILLIONS OF PSI*FT/MIN)	18.72015		18.72015
MAXIMUM FLASH TEMPERATURE		181.3	
MAXIMUM NORMAL LOAD		19.0	
AVERAGE COEFFICIENT OF FRICTION		0.07452	
RPM FOR STRESSES		6000.00	

* * * * * * * * * * * * * * * * * * *

THE EFFECTIVE CONTACT RATIO = 1.4500

* * * * * * * * * * * * * * * * * * *

MAXIMUM VALUES FOR SUN-PLANET MESH 2

	SUN		PLANET
FILLET STRESS CONCENTRATION (KSUBT)	1.45022		1.38394
MAXIMUM HERTZ STRESS	19788.2		19788.2
MAXIMUM HERTZ STRESS AT PD	10664.8		10664.8
MAXIMUM BENDING STRESS	277.4		302.7
MAXIMUM BENDING STRESS AT PD	138.5		69.4
DEPTH TO MAXIMUM SHEAR	0.00041		0.00041
MAXIMUM DYNAMIC PV(MILLIONS OF PSI*FT/MIN)	18.50339		18.50339
MAXIMUM FLASH TEMPERATURE		181.3	
MAXIMUM NORMAL LOAD		19.0	
AVERAGE COEFFICIENT OF FRICTION		0.01432	
RPM FOR STRESSES		6000.00	

* * * * * * * * * * * * * * * * * * *

THE EFFECTIVE CONTACT RATIO = 1.4400

* * * * * * * * * * * * * * * * * * *

MAXIMUM VALUES FOR SUN-PLANET MESH 3

	SUN		PLANET
FILLET STRESS CONCENTRATION (KSUBT)	1.41938		1.41342
MAXIMUM HERTZ STRESS	19863.3		19863.3
MAXIMUM HERTZ STRESS AT PD	13637.9		13637.9
MAXIMUM BENDING STRESS	279.4		305.1
MAXIMUM BENDING STRESS AT PD	171.1		130.3
DEPTH TO MAXIMUM SHEAR	0.00041		0.00041
MAXIMUM DYNAMIC PV(MILLIONS OF PSI*FT/MIN)	18.09996		18.09996
MAXIMUM FLASH TEMPERATURE		181.2	
MAXIMUM NORMAL LOAD		19.2	
AVERAGE COEFFICIENT OF FRICTION		0.01489	
RPM FOR STRESSES		6000.00	

* * * * * * * * * * * * * * * * * * *

THE EFFECTIVE CONTACT RATIO = 1.4500

* * * * * * * * * * * * * * * * * * *

Non-flexible Carrier Results

MAXIMUM VALUES FOR SUN-PLANET MESH 1

	SUN		PLANET
FILLET STRESS CONCENTRATION (KSUBT)	1.43617		1.39553
MAXIMUM HERTZ STRESS	19791.8		19791.8
HERTZ STRESS AT PD	19403.5		19403.5
MAXIMUM BENDING STRESS	278.1		302.8
BENDING STRESS AT PD	259.2		295.7
DEPTH TO MAXIMUM SHEAR	0.00041		0.00041
MAXIMUM DYNAMIC PV(MILLIONS OF PSI*FT/MIN)	18.67369		18.67369
MAXIMUM NORMAL LOAD		19.1	
AVERAGE COEFFICIENT OF FRICTION		0.07450	
RPM FOR STRESSES		6000.00	

* * * * * * * * * * * * * * * * * * *

THE EFFECTIVE CONTACT RATIO = 1.4500

* * * * * * * * * * * * * * * * * * *

MAXIMUM VALUES FOR SUN-PLANET MESH 2

	SUN		PLANET
FILLET STRESS CONCENTRATION (KSUBT)	1.45022		1.38394
MAXIMUM HERTZ STRESS	19835.1		19835.1
HERTZ STRESS AT PD	10676.7		10676.7
MAXIMUM BENDING STRESS	278.8		304.1
BENDING STRESS AT PD	139.8		69.5
DEPTH TO MAXIMUM SHEAR	0.00041		0.00041
MAXIMUM DYNAMIC PV(MILLIONS OF PSI*FT/MIN)	18.40285		18.40285
MAXIMUM NORMAL LOAD		19.1	
AVERAGE COEFFICIENT OF FRICTION		0.01433	
RPM FOR STRESSES		6000.00	

* * * * * * * * * * * * * * * * * * *

THE EFFECTIVE CONTACT RATIO = 1.4400

* * * * * * * * * * * * * * * * * * *

MAXIMUM VALUES FOR SUN-PLANET MESH 3

	SUN		PLANET
FILLET STRESS CONCENTRATION (KSUBT)	1.41938		1.41342
MAXIMUM HERTZ STRESS	19951.9		19951.9
HERTZ STRESS AT PD	13781.5		13781.5
MAXIMUM BENDING STRESS	282.5		307.8
BENDING STRESS AT PD	174.7		133.0
DEPTH TO MAXIMUM SHEAR	0.00041		0.00041
MAXIMUM DYNAMIC PV(MILLIONS OF PSI*FT/MIN)	18.22069		18.22069
MAXIMUM NORMAL LOAD		19.4	
AVERAGE COEFFICIENT OF FRICTION		0.01505	
RPM FOR STRESSES		6000.00	

* * * * * * * * * * * * * * * * * * *

Figure 12b. (cont)

Flexible Carrier Results

MAXIMUM VALUES FOR RING-PLANET MESH 1

	PLANET		RING
FILLET STRESS CONCENTRATION (KSUBT)	1.42396		1.54019
MAXIMUM HERTZ STRESS	12817.4		12817.4
MAXIMUM HERTZ STRESS AT PD	3061.9		3061.9
MAXIMUM BENDING STRESS	297.0		137.2
MAXIMUM BENDING STRESS AT PD	28.7		4.7
DEPTH TO MAXIMUM SHEAR	0.00056		0.00056
MAXIMUM DYNAMIC PV(MILLIONS OF PSI*FT/MIN)	5.75783		5.75783
MAXIMUM FLASH TEMPERATURE		180.3	
MAXIMUM NORMAL LOAD		17.0	
AVERAGE COEFFICIENT OF FRICTION		0.00225	
RPM FOR STRESSES		6000.00	

* * * * * * * * * * * * * * * * * * * *
THE EFFECTIVE CONTACT RATIO = 1.6500
* * * * * * * * * * * * * * * * * * * *

MAXIMUM VALUES FOR RING-PLANET MESH 2

	PLANET		RING
FILLET STRESS CONCENTRATION (KSUBT)	1.44438		1.53765
MAXIMUM HERTZ STRESS	12237.1		12237.1
MAXIMUM HERTZ STRESS AT PD	10957.6		10957.6
MAXIMUM BENDING STRESS	271.1		130.8
MAXIMUM BENDING STRESS AT PD	247.8		84.6
DEPTH TO MAXIMUM SHEAR	0.00054		0.00054
MAXIMUM DYNAMIC PV(MILLIONS OF PSI*FT/MIN)	5.50134		5.50134
MAXIMUM FLASH TEMPERATURE		180.3	
MAXIMUM NORMAL LOAD		15.5	
AVERAGE COEFFICIENT OF FRICTION		0.00907	
RPM FOR STRESSES		6000.00	

* * * * * * * * * * * * * * * * * * * *
THE EFFECTIVE CONTACT RATIO = 1.6300
* * * * * * * * * * * * * * * * * * * *

MAXIMUM VALUES FOR RING-PLANET MESH 3

	PLANET		RING
FILLET STRESS CONCENTRATION (KSUBT)	1.40377		1.55480
MAXIMUM HERTZ STRESS	12601.8		12601.8
MAXIMUM HERTZ STRESS AT PD	0.0		0.0
MAXIMUM BENDING STRESS	292.9		150.3
MAXIMUM BENDING STRESS AT PD	0.0		0.0
DEPTH TO MAXIMUM SHEAR	0.00056		0.00056
MAXIMUM DYNAMIC PV(MILLIONS OF PSI*FT/MIN)	5.83517		5.83517
MAXIMUM FLASH TEMPERATURE		180.4	
MAXIMUM NORMAL LOAD		16.6	
AVERAGE COEFFICIENT OF FRICTION		0.01839	
RPM FOR STRESSES		6000.00	

* * * * * * * * * * * * * * * * * * * *
THE EFFECTIVE CONTACT RATIO = 1.5800
* * * * * * * * * * * * * * * * * * * *

Non-flexible Carrier Results

MAXIMUM VALUES FOR RING-PLANET MESH 1

	PLANET		RING
FILLET STRESS CONCENTRATION (KSUBT)	1.42396		1.54019
MAXIMUM HERTZ STRESS	12713.6		12713.6
HERTZ STRESS AT PD	3373.3		3373.3
MAXIMUM BENDING STRESS	294.8		140.2
BENDING STRESS AT PD	34.8		5.8
DEPTH TO MAXIMUM SHEAR	0.00056		0.00056
MAXIMUM DYNAMIC PV(MILLIONS OF PSI*FT/MIN)	5.80285		5.80285
MAXIMUM NORMAL LOAD		16.8	
AVERAGE COEFFICIENT OF FRICTION		0.00267	
RPM FOR STRESSES		6000.00	

* * * * * * * * * * * * * * * * * * * *
THE EFFECTIVE CONTACT RATIO = 1.6400
* * * * * * * * * * * * * * * * * * * *

MAXIMUM VALUES FOR RING-PLANET MESH 2

	PLANET		RING
FILLET STRESS CONCENTRATION (KSUBT)	1.44438		1.53765
MAXIMUM HERTZ STRESS	12391.7		12391.7
HERTZ STRESS AT PD	11059.1		11059.1
MAXIMUM BENDING STRESS	275.2		128.5
BENDING STRESS AT PD	252.4		86.2
DEPTH TO MAXIMUM SHEAR	0.00054		0.00054
MAXIMUM DYNAMIC PV(MILLIONS OF PSI*FT/MIN)	5.50748		5.50748
MAXIMUM NORMAL LOAD		15.9	
AVERAGE COEFFICIENT OF FRICTION		0.00396	
RPM FOR STRESSES		6000.00	

* * * * * * * * * * * * * * * * * * * *
THE EFFECTIVE CONTACT RATIO = 1.6400
* * * * * * * * * * * * * * * * * * * *

MAXIMUM VALUES FOR RING-PLANET MESH 3

	PLANET		RING
FILLET STRESS CONCENTRATION (KSUDT)	1.40377		1.55480
MAXIMUM HERTZ STRESS	12458.3		12453.3
HERTZ STRESS AT PD	0.0		0.0
MAXIMUM BENDING STRESS	283.1		146.4
BENDING STRESS AT PD	0.0		0.0
DEPTH TO MAXIMUM SHEAR	0.00055		0.00055
MAXIMUM DYNAMIC PV(MILLIONS OF PSI*FT/MIN)	5.73373		5.73373
MAXIMUM NORMAL LOAD		16.1	
AVERAGE COEFFICIENT OF FRICTION		0.01038	
RPM FOR STRESSES		6000.00	

ORIGINAL PAGE IS
OF POOR QUALITY

ORIGINAL PAGE IS
OF POOR QUALITY

Figure 13a. Non-flexible Carrier Gear Mesh Plots

PV = pressure sliding velocity

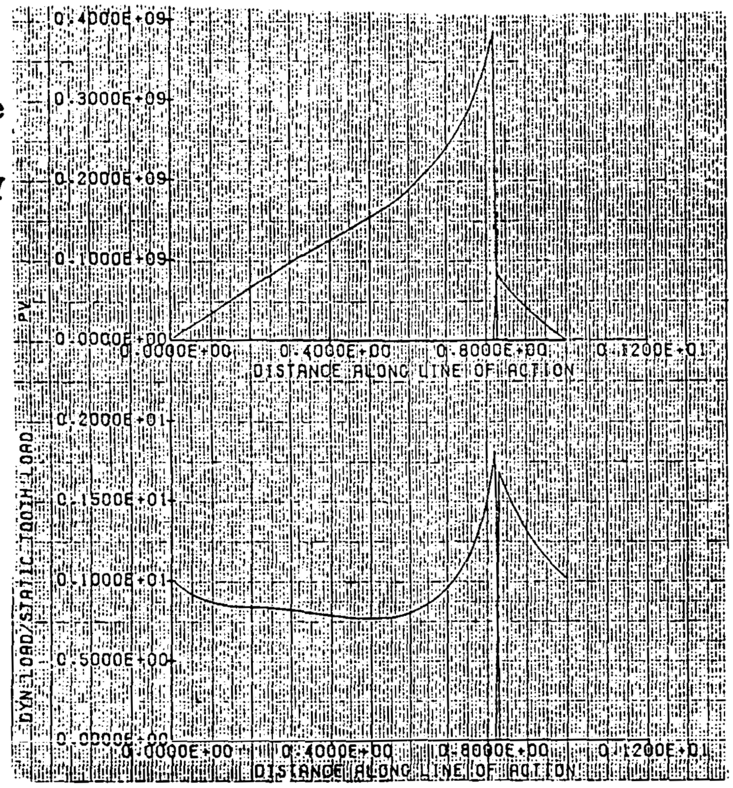

sun-planet mesh

pitch point - 0.0 distance along line of action

°F

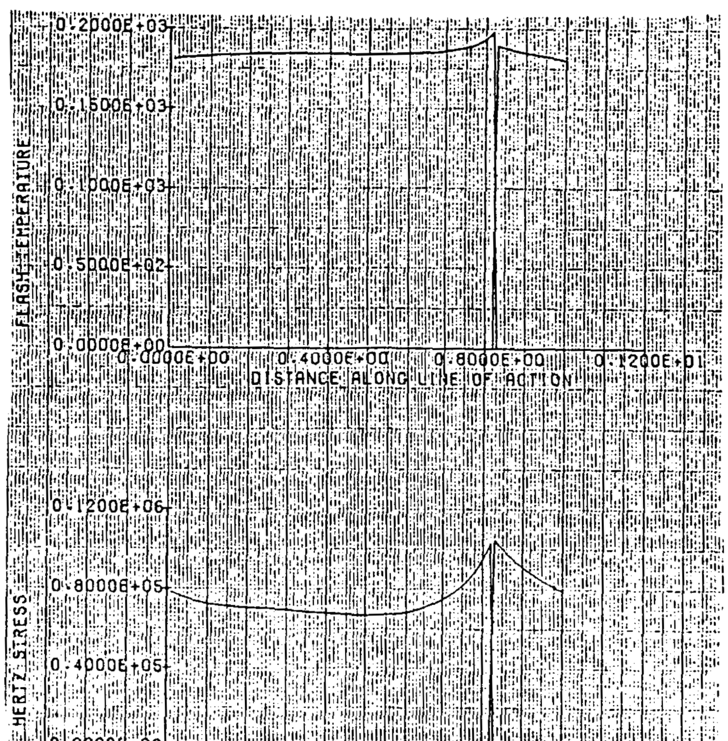

sun-planet mesh

psi

Figure 13a (cont)

psi

psi

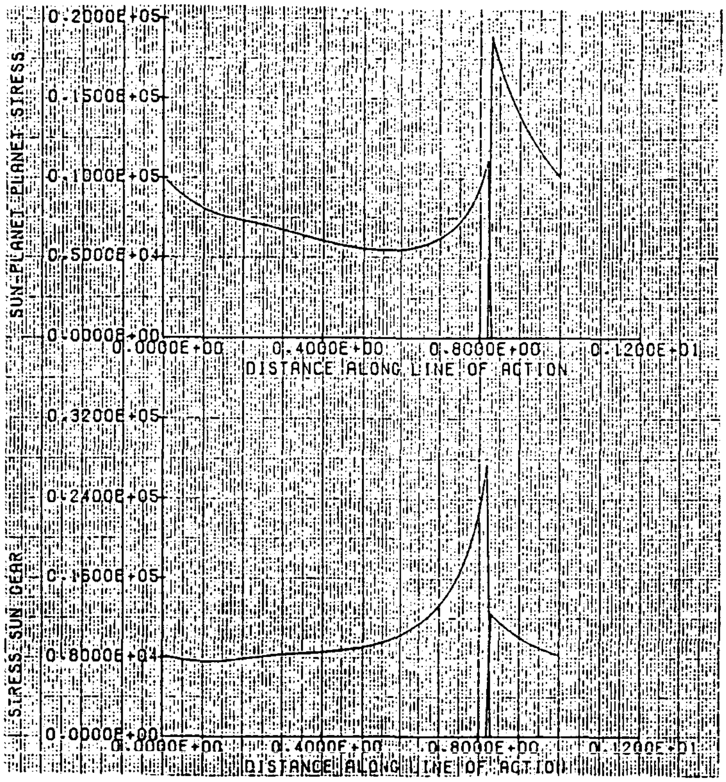

sun-planet mesh

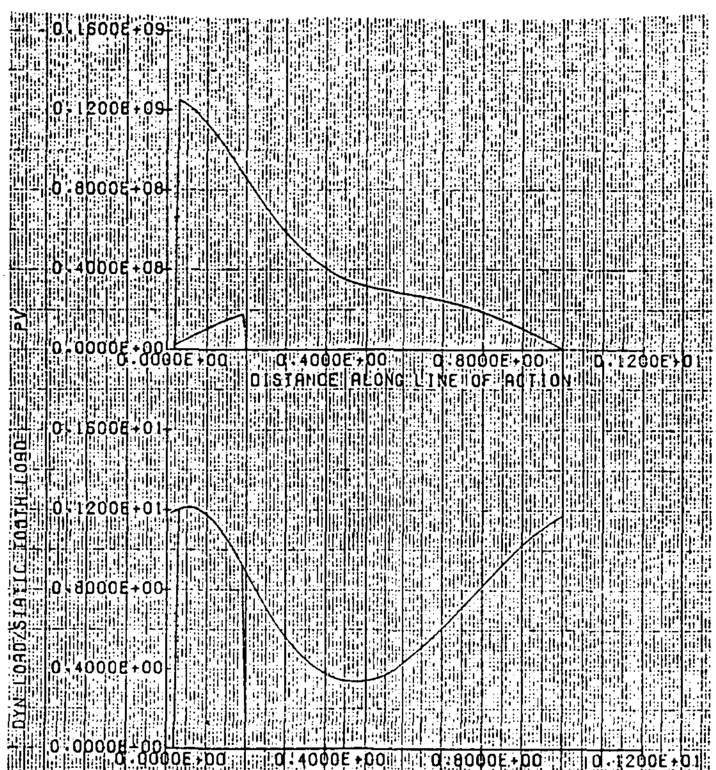

ring-planet mesh

Figure 13a (cont)

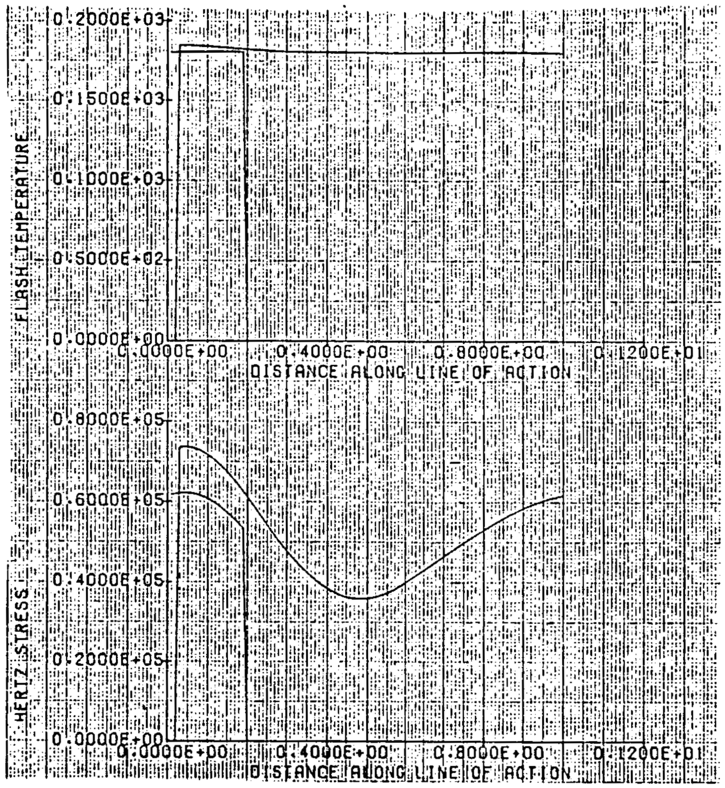

ring-planet mesh

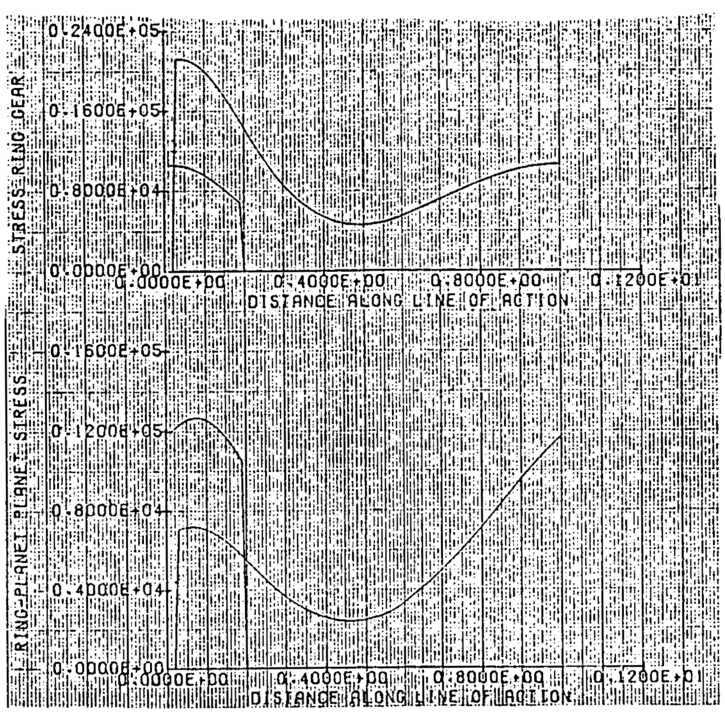

ring-planet mesh

Figure 13b. Flexible Carrier Gear Mesh Plots

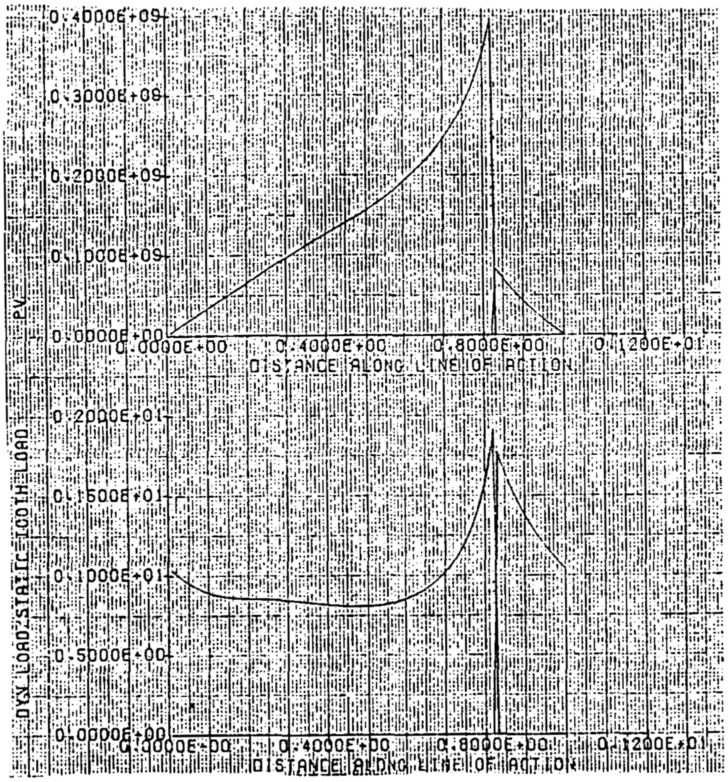

sun-planet mesh

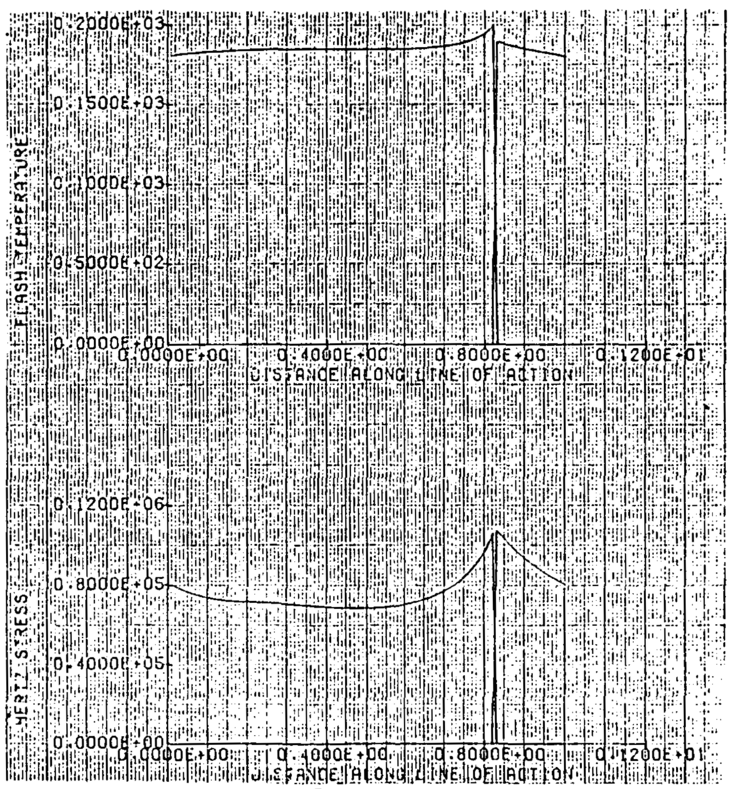

sun-planet mesh

Figure 13b (cont)

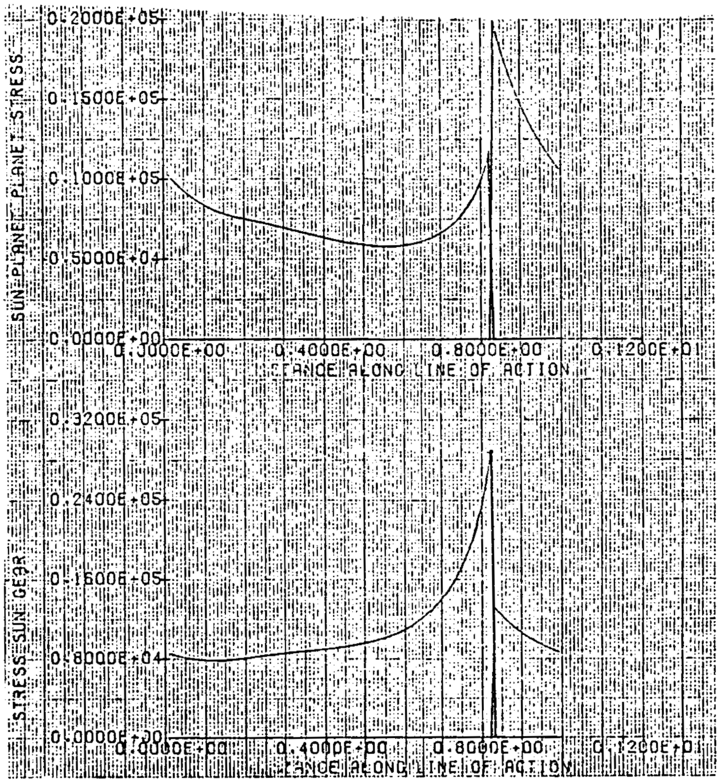

sun-planet mesh

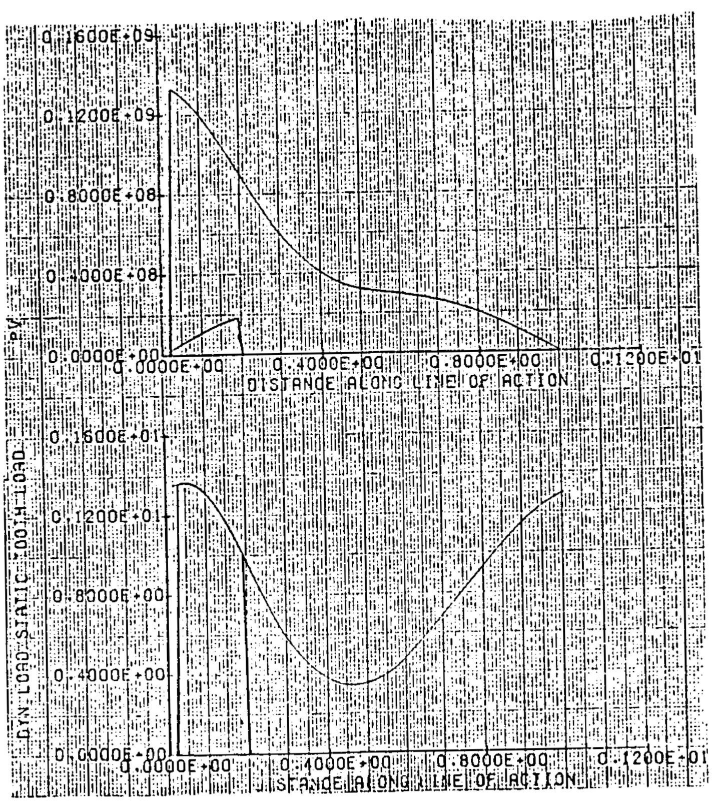

ring-planet mesh

Figure 13b (cont)

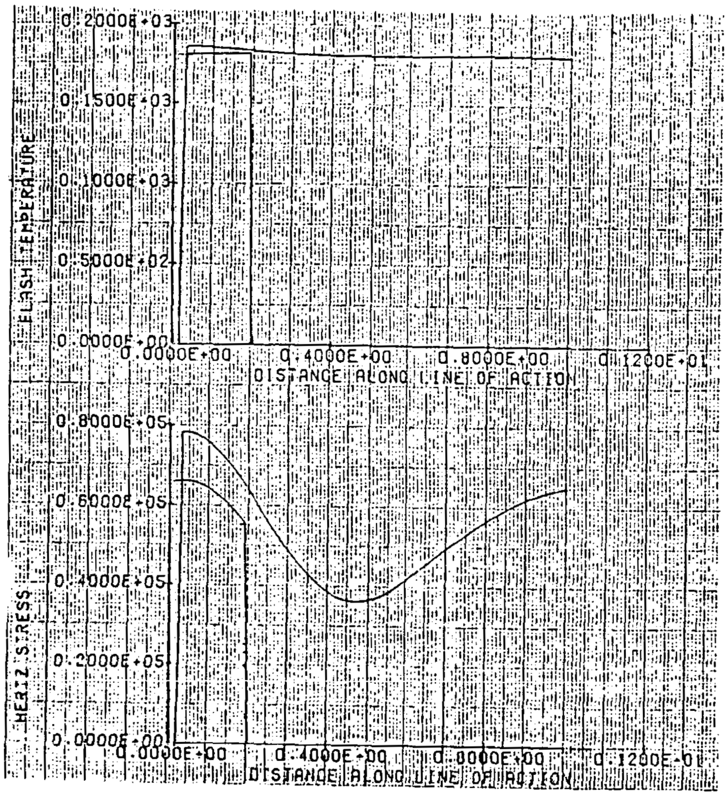

ring-planet mesh

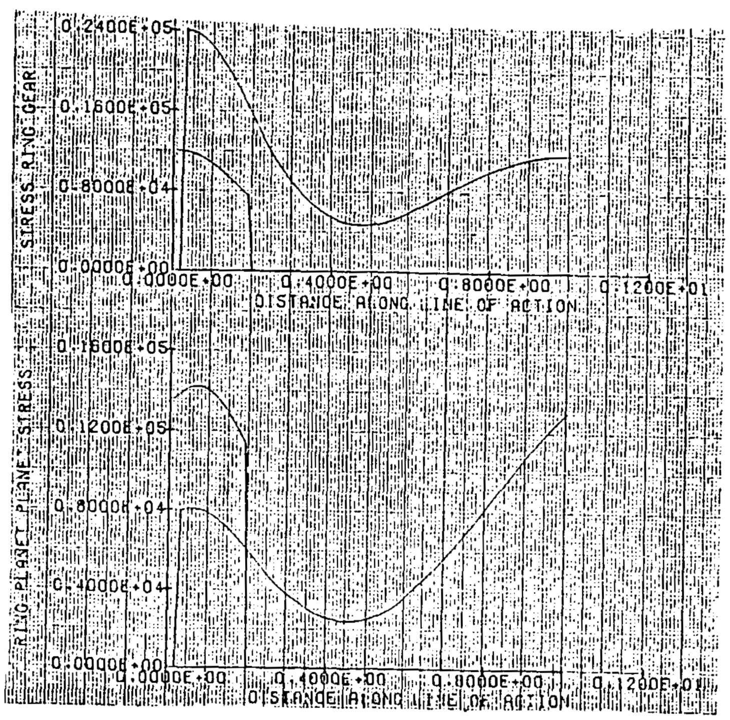

ring-planet mesh

XII. APPENDICES

APPENDIX A: USER'S MANUAL

Part 1: Summary of New Option Information

The new options can be easily added to any existing data set. The new inputs corresponding to the new options are summarized below. An updated version of the User's Manual of Reference 1 follows in Part 2 with all the input descriptions. In addition, some comments are included that may be useful for input or interpretation of output. It should be noted that the locations to request plots have been changed.

Floating Sun:

Springrates (locations 115 and 116) and damping (locations 117 and 118) are input for two Cartesian directions, horizontal and vertical or x and y , at the sun center. The translational mass of the sun gear (location 119) and the additional boundary conditions (locations 561 to 644) are also inputs. The additional boundary conditions that must be input are for the sun center and the carrier or ring displacements and velocities, see the updated location listing, Part 2, for details on input.

Note that some damping should be input or numerical instabilities may develop.

The convergence criteria should not initially be too stringent, especially if the spring rates at the sun center are soft. This can lead to diverging boundary conditions, especially for systems with unequal phasing constants.

Natural Frequencies:

The user can utilize existing input data sets by simply adding a trigger (location 805). In general, minimum input (Level I) is all that is necessary; however, any existing data set can be used with the addition of the trigger. The trigger is also used to indicate the type of output -- frequencies only or eigenvalues/eigenvectors, etc. After the frequencies have been calculated, the program ends and does not continue with the dynamic solution.

A list of the various system types that can be investigated and the corresponding number of degrees of freedom follows.

k = type of epicyclic spur gear system
n = number of planets
ndf = number of degrees of freedom

k = 1 planetary system, i.e. ring gear fixed and rigid planet carrier
ndf = n + 2

k = 2 star system, i.e. planet carrier fixed and rigid ring gear rim
ndf = n + 2

k = 3 differential system, i.e. rigid ring gear rim and rigid planet carrier
ndf = n + 3

k = 4 single mesh, sun-planet(s) or external/external mesh
ndf = n + 1

k = 5 single mesh, ring-planet(s) or external/internal
ndf = n + 1

k = 6 planetary system with flexible carrier
ndf = 2*n + 1

k = 7 star system with flexible ring gear
ndf = 2*n + 1

k = 8 * differential system with both flexibar and flexible planet carrier
ndf = 3*n + 1

*NOTE: For k=8, a differential system with both a flexible carrier and a flexible ring, there is only a natural frequency solution, i.e. there is no dynamic solution.

To include the floating sun option or for systems with k of 6, 7, or 8, note that the corresponding additional parameters must be input, eg. the floating sun mass and sun center springs. Two additional degrees of freedom are added to any system if the floating sun parameters are input.

<u>Phasing constants for mesh time location simulation:</u>

For a phasing constant of 0 the stiffnesses will be at the pitch diameter or time zero, while for a phasing constant of 1, the stiffnesses will again be at the pitch diameter but at the end of the meshing time. Thus, for phasing constants between 0 and 1, the teeth will be located at a corresponding percentage of the total mesh time.

Other program inputs affecting the output:

The normalized eigenvectors or mode shapes can be printed if desired. These will indicate displacements along the lines of action for the rotational modes, which are all modes except when there is a floating sun. The additional equations for the floating sun are for translational movement of the sun center in the x and y directions and will lead to translational modes.

If the full output is requested, the user may find rigid body modes that do not always correspond to a natural frequency of exactly zero, but are several orders of magnitude less than the actual frequencies and are the first frequencies output. This is caused by the numerical eigenvalue/eigenvector solution.

Systems 6,7 and 8 may yield rigid body modes if the stiffnesses for the carrier and/or ring gear rim or pin stiffnesses are insufficient. For these situations either the carrier and/or the ring are acting as rigid bodies. For these systems all the frequencies are output, but if the first two frequencies are orders of magnitude less than the other frequencies, the pin stiffnesses and the results should be carefully examined.

Input geometry can affect the tooth pair stiffnesses, as well as the input torque.

Finite Element Helical Gear Tooth Analysis:

This option is initiated by a trigger in location 111. Note that the default for helical gear tooth analysis is 0., or the original option of 10 independent axial segments, and that no provision is made for double helical tooth forms in the finite element solution.

Another point of interest is the numerical solution stability. The size of the mesh time step has an effect on the numerical solution. This is currently set to be equal to the total mesh time divided by 100 for spur gears and the finite element helical option. For the original helical option the total mesh time is divided by 10. For very low rpms this time step can become relatively large and could lead to an unstable solution.

Flexible Carrier or Flexible Ring Gear Rim Option:

The flexible carrier/ring gear rim option is triggered by the input system type, for either a planetary or star system. The additional inputs required are stiffnesses (locations 800-803) In addition, the boundary conditions must now be input for each individual component (locations 481 to 621). The following procedure is recommended to reduce the iterations for convergence:

1. Run the case without a flexible carrier or ring gear rim (k = 1 or 2).

2. Estimate the carrier segment or ring gear rim displacement (assuming equal segment displacements) from :

$$XCO(I) = \frac{\text{total output torque}}{(\text{carrier base radius * pin stiffness})}$$

or:

$$XRO(I) = \frac{\text{total output torque}}{(\text{ring gear base radius * pin stiffness})}$$

3. Using the converged displacement boundary conditions from Step 1, solve for the remaining displacements recalling the following tooth pair displacement (along the line of action) relationships:

XOSP(I) = XSO - XPO(I) - XCO(I)

XORP(I) = XPO(I) - XCO(I) - XRO(I)

Recall that for planetary systems XRO(I) = 0. and for star systems, XCO(I) = 0.

4. For the initial velocity conditions, one value must be assumed (e.g. carrier velocity = 0.) as there are two equations and three unknowns. The same relations hold as in Step 3 replacing the displacements with velocities.

Part 2: List of Input Variables and Corresponding Location Numbers

* *
* * * * * * * * * * * F 1 7 8 * * * * * * * * * * * * * * * * * *
* *
* * U S E R ' S M A N U A L F O R M U L T I P L E M E S H *
* * S P U R A N D H E L I C A L G E A R S Y S T E M S * * *
* *
* * * * * * * * * * JUNE 1986 * * * * * * * * * * * * * * *
* *

* * * * * * * * * PROGRAM RESTRICTIONS * * * * * * * * * * * * * *

1. MAXIMUM PLANETS FOR SPUR AND SINGLE HELICAL GEARING IS 20
2. MAXIMUM PLANETS FOR DOUBLE HELICAL GEARING IS 10
3. MAXIMUM ITERATIONS FOR SOLUTION CONVERGENCE IS 20
4. MAXIMUM TEETH WITH TOOTH SPACING ERRORS IS 5
5. 10 TEETH ARE CHECKED FOR DYNAMICS DURING TOOTH ERROR PASS
6. MAXIMUM INVOLUTE CONTACT RATIO IS 3.0
7. MAXIMUM NUMBER OF SUN TEETH IS 50 FOR RUNOUT OPTION

* *
* * *INPUT DATA FOR MULTIPLE MESH SPUR AND HELICAL GEAR PROGRAM * * *

NOTE: ALL GEOMETRIC INPUT DATA IS IN THE ROTATIONAL PLANE AND ALL DEFAULT VALUES ARE 0.0 UNLESS OTHERWISE NOTED.

ANGLES ARE IN DEGREES
FORCES ARE IN POUNDS (#)
LENGTHS ARE IN INCHES (IN)
MASSES ARE IN (#-SEC**2/IN)
STRESSES ARE IN (#/IN**2)
TEMPERATURES ARE IN DEGREES FAHRENHEIT

THE DATA SET REQUIRED TO RUN THE MULTIPLE MESH PROGRAM IS DESCRIBED BELOW AND AN EXAMPLE DATA SET WITH CORRESPONDING EXAMPLE PROBLEM ARE IN APPENDIX C, 1984 MULTIPLE MESH REPORT NASA CR-174747. A LIST OF GEAR SYSTEM PARAMETERS WITH DESCRIPTIONS, LOCATION NUMBERS, AND SOME NONZERO DEFAULT VALUES FOLLOW THE INPUT DESCRIPTION.

CARD 1: TITLE CARD—CONTAINS CASE TITLE AND/OR DESCRIPTIVE
(LINE 1) INFORMATION. AT LEAST ONE COLUMN FROM 1 TO 40 MUST BE NONBLANK.

DATA CARDS: CARDS CONTAIN DATA IN THE FORM SHOWN IN FIGURE 1. FROM LEFT TO RIGHT THE INPUTS ARE: NUMBER OF DATA ITEMS ON CARD, LOCATION NUMBER OF FIRST DATA ITEM IN LINE (SEE GEAR SYSTEM PARAMETERS SECTION FOR LOCATION NUMBERS AND CORRESPONDING PARAMETER

DESCRIPTIONS), AND DATA ITEMS ARE IN 5 FIELDS OF 12 SPACES.

CASE TERMINATION CARD: TO TERMINATE A CASE THE LAST LINE MUST CONTAIN 0-1. IN COLUMNS 1-4.

SUBSEQUENT CASES: ANOTHER DATA SET OF THE SAME FORMAT—TITLE CARD, DATA CARDS, AND CASE TERMINATION CARD —MAY FOLLOW THE CASE TERMINATION CARD.

JOB TERMINATION CARD: AFTER THE LAST SUBSEQUENT CASE TERMINATION CARD, A BLANK CARD (LINE) MUST BE INCLUDED, OTHERWISE AN ERROR MESSAGE IS GENERATED.

** NOTE ** ALL NUMBERS MUST BE REAL EXCEPT THE NUMBER OF ITEMS, THAT IS, A DECIMAL POINT MUST BE INCLUDED. IT IS NOT NECESSARY TO INPUT ZERO VALUES AS THEY WILL DEFAULT TO ZERO UNLESS OTHERWISE SPECIFIED.

A BRIEF DESCRIPTION OF OUTPUT FOLLOWS THE GEAR SYSTEM PARAMETER SECTION.

*** THE FOLLOWING EXAMPLE IS FROM THE 1984 NASA CR ***
IN APPENDIX C THE TITLE CARD READS 'EXAMPLE DATA SET'. THE NEXT LINE IN THE DATA SET CONTAINS, FROM LEFT TO RIGHT, 5, CORRESPONDING TO THE FIVE DATA ITEMS ON TO BE ON THAT LINE, THEN THE LOCATION NUMBER (1.) CORRESPONDING TO THE FIRST INPUT DATA TO BE PUT IN COLUMNS 13-24, FOLLOWED BY THE DATA ITEMS: LEVEL (2.), THE DIAMETRAL PITCH (8.4667), THE PRESSURE ANGLE (22.5), COAST SIDE PRESSURE ANGLE AND HELIX ANGLE.(BOTH COAST SIDE PRESSURE ANGLE AND HELIX ANGLE = 0 FOR STANDARD SPUR GEARS AND WOULD DEFAULT TO 0 IF LEFT BLANK)

MOST OF THE INPUT VARIABLES HAVE SUFFICIENT EXPLANATION IN THE GEAR SYSTEM PARAMETERS SECTION, HOWEVER THE FOLLOWING PARAMETERS SHOULD BE CALCULATED AS FOLLOWS.

*** EQUIVALENT MASSES:

SUN EQUIVALENT MASS = J / (BASE RADIUS OF SUN)**2

WHERE J IS THE MASS MOMENT OF INERTIA FOR THE SUN. THE OTHER COMPONENTS ARE CALCULATED SIMILARLY, USING THE CORRESPONDING MOMENTS AND BASE RADII.

*** PHASING CONSTANTS:

FOR EQUALLY SPACED PLANETS THE SUN PHASING CONSTANTS ARE DETERMINED BY ASSUMING THE FIRST PLANET MESH HAS A PHASING

CONSTANT OF ZERO. THE REMAINING SUN-PLANET PHASING CONSTANTS ARE DETERMINED BY:

(PLANET # - 1)*THE FRACTIONAL REMAINDER FROM DIVIDING THE
NUMBER OF SUN TEETH BY THE TOTAL NUMBER OF PLANETS
WHERE THE 'FRACTIONAL REMAINDER' INDICATES THE SPACING DIFFERENCE BETWEEN PLANETS.

THE PHASING CONSTANTS FOR THE RING-PLANET MESHES ARE DETERMINED THE SAME WAY IF THE PLANET HAS AN ODD NUMBER OF TEETH, USING THE NUMBER OF RING TEETH. IF THE PLANETS HAVE AN EVEN NUMBER OF TEETH THE CONSTANTS ARE CALCULATED FOR THE SUN MESHES THEN 0.5 IS ADDED TO EACH TO OBTAIN THE RING-PLANET MESH PHASING CONSTANTS (KRP), DUE TO THE RING GEAR BEING .5 OFFSET FROM THE SUN GEAR.

EXAMPLE CORRESPONDING TO APPENDIX C:

SUN PLANET MESH— 14/3 = 12 2/3

PLANET 1, KSP(1) = 0.

PLANET 2, (2-1)*(2/3) = .6666667
KSP(2) = .6666667

PLANET 3, (3-1)*(2/3)=1.3333333
KSP(3) = .3333333

RING PLANET MESH— (EVEN NUMBER OF PLANET TEETH)

PLANET 1, KRP(1) = KSP(1) + .5 = .5

PLANET 2, KSP(2) + .5 = 1.1666667
KRP(2) = .1666667

PLANET 3, KSP(3) + .5 = .8333333

KRP(3) = .8333333

*** BOUNDARY CONDITIONS:

AN INITIAL ESTIMATE FOR DISPLACEMENT BOUNDARY CONDITIONS MAY BE OBTAINED BY DIVIDING THE STATIC TOOTH LOAD AT THE PITCH RADIUS BY THE TOOTH SPRING RATE AT THE PITCH RADIUS.

%%*%*%*%*%*%*% 1986 UPDATE *%*%*%*%*%*%*%*%*%*%

SEE THE 1986 CR REPORT FOR A SUMMARY OF THE LOCATIONS FOR THE ADDITIONAL INPUTS REQUIRED FOR THE NEW OPTIONS. THE SAME LEVELS APPLY, WHERE THE NEW OPTIONS CAN BE USED WITH ANY LEVEL OF INPUT. NOTE THAT THE LOCATIONS TO TRIGGER THE PLOTS HAVE BEEN CHANGED. ALSO NOTE THAT THE NEW OPTIONS THAT ADD DEGREES OF FREEDOM ARE SENSITIVE TO THE INITIAL BOUNDARY CONDITIONS, SEE CR FOR INITIAL FLEXIBLE CARRIER BOUNDARY CONDITION INPUT RECOMMENDATIONS.

%

***** LEVELS OF INPUT

LEVEL I INPUT

THE FIRST INPUT ITEM WILL BE THE LEVEL DESIRED, FOLLOWED BY ITEMS 2 THROUGH 51 AND WHERE NOTED. THE OTHER VALUES WILL DEFAULT. THE MATERIAL PROPERTIES, LOCATIONS 22 TO 27, DEFAULT FOR STEEL. THE TOLERANCES ARE SET TO ZERO OR DEFAULT VALUES BELOW, ERRORS ARE SET TO 0. THERE ARE NO PROFILE MODIFICATIONS. OTHER NONZERO DEFAULT VALUES ARE:

SURFACE ROUGHNESS - 25
OIL TEMPERATURE - 180 F
MATERIAL CONSTANT - 0.0528
DAMPING - .02
OIL TYPE MIL-L-23699

ANY DESIRED PLOTS CAN BE OBTAINED, SEE LOC 651-658,
A CHECK ON INPUT DATA CAN BE MADE, LOC # 699.
IF CONTACT RATIO IS HIGH (GREATER THAN 2) IT MUST BE INPUT IN LOC 54 & 55.

LEVEL II INPUT

THE MINIMUM INPUT FOR THIS LEVEL WOULD BE LEVEL 1 DATA PLUS DAMPING, FLASH TEMPERATURE DATA, SOLUTION ITERATION DATA, AND PHASING CONSTANTS. DEFAULT VALUES ARE ZERO UNLESS INDICATED OTHERWISE BELOW. THE MAXIMUM INPUT WOULD INCLUDE THE ITEMS REQUIRED FOR LEVEL 1 PLUS ALL OTHER ITEMS EXCEPT LOCATIONS 64, 65, 91-100, AND 175-192.

LEVEL III INPUT

LEVEL 3 REQUIRES ALL ITEMS TO BE INPUT, UNLESS DEFAULT VALUES ARE INDICATED BELOW. THE MINIMUM INPUT FOR THIS LEVEL WOULD BE LEVEL 2 DATA.

**** NOTE: FOR HIGH CONTACT RATIO GEARS (CR > 2.), THE USER MUST INPUT THE CR (LOC 54 AND 55). THE PROGRAM CALCULATES RATIO IF CR < 2.

```
*** G E A R   S Y S T E M   P A R A M E T E R S  *****************

 LOC  NAME    DESCRIPTION
* * * * * * * * * * * * * * * * * * * * * * * * * * * * * * * * * * *

  1   LEVEL   TRIGGER FOR LEVEL OF INPUT DATA
  2   DP      DIAMETRAL PITCH (NORMAL PLANE)
  3   PSANG   SUN-PLANET DRIVE SIDE PRESSURE ANGLE @ PD
              RING-PLANET COAST SIDE PRESSURE ANGLE @ PD
  4   PSANGB  SUN-PLANET COAST SIDE PRESSURE ANGLE @ PD
              RING-PLANET DRIVE SIDE PRESSURE ANGLE @ PD
              ** 0.0 IF PRESSURE ANGLES FOR DRIVE & COAST SIDES EQUAL
  5   PSIO    HELIX ANGLE @ PD
              ** 0.0 FOR SPUR GEARS
  6   N1      NUMBER OF TEETH ON SUN GEAR
  7   N2                         PLANET GEARS
  8   N3                         RING GEAR
  9   FW1     AXIAL FACE WIDTH OF SUN GEAR
 10   FW2                         PLANET GEARS
 11   FW3                         RING GEAR
 12   N       NUMBER OF PLANET GEARS
 13   K       IF K=1 PLANETARY SYSTEM,I.E.,RING GEAR FIXED
              IF K=2 STAR SYSTEM,I.E.,PLANET CARRIER FIXED
          *** IF K=3 DIFFERENTIAL SYSTEM,I.E. NEITHER RING OR CARRIER
                     FIXED
        %% ** IF K=4 NON PLANETARY,I.E., NO RING AND NO CARRIER
                                         SUN-INPUT, PLANET-OUTPUT
        %%    IF K=5 NON PLANETARY,I.E., NO SUN AND NO CARRIER,
                                         PLANET INPUT, RING OUTPUT
            * IF K=6 PLANETARY SYSTEM WITH FLEXIBLE PLANET CARRIER
            * IF K=7 STAR SYSTEM WITH FLEXIBLE RING GEAR RIM

       ******* K = 6 AND K = 7 CURRENTLY UNSTABLE RESULTS ******

            * IF K=6 OR K=7 LOC 88 & 89 ARE REQUIRED FOR PLANET
              CARRIER OR RING GEAR RIM STIFFNESS VALUE ALONG THE
              LINE-OF-ACTION AND AN INTERFACE STIFFNESS.
           ** FOR K=4 AND RUNOUT ERROR, INPUT LOC 200.
          *** FOR K=3, INPUT LOC 18 - 21.
          %%  FOR K=4 OR 5, THE SINGLE MESH PROGRAM WILL GIVE THE
              RESULTS IN LESS CPU TIME DUE TO AN EXACT SOLUTION.
              ALSO, FOR K = 5, THERE IS A  BUG IN THE DEPTH TO MAX
              SHEAR CALCULATION IN THE MULTI-MESH PROGRAM.

 14   TORQ    AXIAL INPUT TORQUE ON SUN GEAR (OR PLANET IF K=5)
 15   RPM     INITIAL AXIAL ROTATIONAL SPEED OF SUN GEAR
                                               (OR PLANET IF K=5)
 16   RPMF    FINAL AXIAL ROTATIONAL SPEED OF SUN GEAR FOR SPD RANGE
 17   INTVL   NUMBER OF MAIN INTERVALS THE SPEED RANGE DIVIDED INTO
              ** FOR ONE RPM ONLY, RPM=RPMF AND INTVL=1.**
```

```
                     STEP SIZE =(RPMF - RPM)/INTVL, THIS STEP SIZE WILL
                     BE AUTOMATICALLY BY 5 IN AREAS OF PEAK LOADS, THUS
                     REFINING THE INCREMENT.

******* DIFFERENTIAL SYSTEM INPUTS ****************************

   18   TOUTC    OUTPUT TORQUE FROM CARRIER
   19   TOUTR    OUTPUT TORQUE FROM RING
   20   RPMC     CARRIER RPM
   21   RPMR     RING RPM

******* GEAR MATERIAL PROPERTIES ******************************

   22   E1       YOUNGS MODULUS * E-06 OF SUN GEAR     (DEFAULT = 30.)
   23   E2                                PLANET GEARS     "    "  "
   24   E3                                RING GEAR        "    "  "
   25   MU1      POISSONS RATIO OF SUN GEAR            (DEFAULT = .30)
   26   MU2                        PLANET GEARS            "    "  "
   27   MU3                        RING GEAR               "    "  "

******* GEAR EQUIVALENT MASSES ********************************

   28   MS       EQUIVALENT MASS OF SUN GEAR ABOUT ROTATIONAL AXIS
   29   MC                          PLANET CARRIER
   30   MR                          RING GEAR

 31-50 MP(I)                        PLANET GEARS
           I - PLANET NUMBER
              *** NOTE: FOR K=6 OR K=7,CARRIER OR RING MASS FOR TOTAL
                        UNIT, NOT SEGMENTS.

******* TRIGGER FOR DOUBLE HELICAL GEARING ********************

   51   DBHEL    IF = 0.0 SINGLE HELICAL GEARING IF PSIO .NE. 0.0
                 IF = 1.0 DOUBLE HELICAL GEARING IF PSIO .NE. 0.0


 * * * * * * * * * * * * * * * * * * * * * * * * * * * * * * * *
            END OF LEVEL 1 INPUT (UNLESS HIGH CONTACT RATIO)
 * * * * * * * * * * * * * * * * * * * * * * * * * * * * * * * *

******* GEAR MESHING DAMPING RATIOS ***************************

   52   ZSP      DAMPING RATIO OF SUN-PLANET MESHES
   53   ZRP         "      "    " RING-PLANET MESHES
 * * * NOTE:  IF CONTACT RATIO > 2, CRSP AND CRRP MUST BE INPUT, BUT
                     THE PROGRAM WILL CALCULATE FOR CR < 2 ONLY.
   54   CRSP     INVOLUTE CONTACT RATIO OF SUN-PLANET MESHES
   55   CRRP        "        "        "   "  RING-PLANET MESHES
```

```
******* ACTIVE FACE WIDTH VALUES ********************************

  **NOTE:  LOC 56 - 59 FOR HELICAL GEARS ONLY, NOT NECESSARY FOR
                          FINITE ELEMENT OPTION
   56    L1SP     INACTIVE SUN-PLANET FACE WIDTH ON LEFT
   57    L2SP         "     "    "     "     "    " RIGHT
   58    L1RP     INACTIVE RING-PLANET FACE WIDTH ON LEFT
   59    L2RP         "     "    "     "     "    " RIGHT

******* SUN-PLANET PROFILE MODIFICATION INPUT DATA *************

   LOCATIONS 66- 68 AND 75-78 ARE ONLY USED FOR PROFILE MODIFICATION
    TABLES, THEY ARE NOT USED IN THE DYNAMICS.

   60    PCTSOD   SD AS A PERCENT OF SOD (%)
   61    PCTSOE   SE AS A PERCENT OF SOE (%)
   62    DELD     DISENGAGEMENT TIP RELIEF (IN.), MINIMUM
   63    DELE     ENGAGEMENT TIP RELIEF    (IN.), MINIMUM
   **NOTE:  SIGN CONVENTION—POSITIVE INPUT, MATERIAL REMOVED

 * * * * * * XNVDX AND XNVEX ARE NOT REQUIRED FOR LEVEL 2 * * * *
   64    XNVDX    DISENGAGEMENT PROFILE MODIFICATION SHAPE FACTOR
   65    XNVEX       ENGAGEMENT
 * * * * * * * * * * * * * * * * * * * * * * * * * * * * * * * *

   66    PMODSP   PERCENT OF TIP RELIEF ON SUN GEAR, ENGAGEMENT
   67    PMDSPD   PERCENT OF TIP RELIEF ON SUN GEAR, DISENGAGEMENT
                    - % TIP RELIEF ON PLANET

   68    DLSP     TOLERANCE AT START OF PROFILE MODIFICATION
   78    DLTOL    TOTAL TIP RELIEF TOLERANCE (SUN + PLANET
                  AND/OR RING + PLANET, DEPENDING ON SYSTEM TYPE)
         SOD - LENGTH OF DISENGAGEMENT PART OF THE LINE OF ACTION
         SOE -    "   "  ENGAGEMENT       "  "  "  "  "    "
         SD & SE ARE THE SEGMENTS OF THE SOD & SOE THAT ARE USED, WHEN
          PROFILE MODIFICATIONS ARE MADE.

******* RING-PLANET PROFILE MODIFICATION INPUT DATA ************

   69    PTSOD3   SD AS A PERCENT OF SOD
   70    PTSOE3   SE AS A PERCENT OF SOE
   71    DELD3    DISENGAGEMENT TIP RELIEF
   72    DELE3    ENGAGEMENT TIP RELIEF

 * * * * * LOCATION 73 AND 74 NOT REQUIRED FOR LEVEL 2 * * * * *
   73    XNVDX3   DISENGAGEMENT PROFILE MODIFICATION SHAPE FACTOR
   74    XNVEX3   ENGAGEMENT PROFILE MODIFICATION SHAPE FACTOR
 * * * * * * * * * * * * * * * * * * * * * * * * * * * * * * *

   75    PMODRP   PERCENT OF TIP RELIEF ON PLANET GEAR, ENGAGEMENT
```

76	PMDRPD	PERCENT OF TIP RELIEF ON PLANET GEAR, DISENGAGEMENT = % TIP RELIEF ON RING GEAR
77	DLRP	TOLERANCE AT START OF PROFILE MODIFICATION
78	DLTOL	TOTAL TIP RELIEF TOLERANCE, FOR BOTH SUN+PLANET AND/OR RING + PLANET

****** MESH MODIFICATION DUE TO FACE WIDTH CROWNING ***********

80	LECSP	LENGTH OF FACE WIDTH CROWN OF ENGAGEMENT FOR SP MESH
81	LDCSP	" " " " " " DISENGAGEMENT FOR SP MESH
82	DLECSP	ENGAGEMENT EDGE RELIEF FOR SP MESH
83	DLDCSP	DISENGAGEMENT EDGE RELIEF FOR SP MESH
84	LECRP	LENGTH OF FACE WIDTH CROWN OF ENGAGEMENT FOR RP MESH
85	LDCRP	" " " " " " DISENGAGEMENT FOR RP MESH
86	DLECRP	ENGAGEMENT EDGE RELIEF FOR RP MESH
87	DLDCRP	DISENGAGEMENT EDGE RELIEF FOR RP MESH

****** TOOTH PAIR COMPLIANCE DATA *****************************

90	WIOK	IF = 0.0 PREPROCESSOR CALULATES TOOTH PAIR COMPLIANCE IF = 1.0 INPUT COMPLIANCE DATA IN LOCATIONS 91-101

(FOR FINITE ELEMENT HELICAL COMPLIANCE, LOC 111)

* * * * * 91 - 100 NOT REQUIRED FOR LEVEL 2 * * * * * * * * * * * * *

91	SPKSP	SINGLE TOOTH PAIR SPRINGRATE OF SUN-PLANET MESHES
92	COMASP	COMPLIANCE CONSTANT (S/SO)**1 OF SUN-PLANET MESHES
93	COMBSP	2
94	COMCSP	3
95	COMDSP	4
96	SPKRP	SINGLE TOOTH PAIR SPRINGRATE OF RING-PLANET MESHES
97	COMARP	COMPLIANCE CONSTANT (S/SO)**1 OF RING-PLANET MESHES
98	COMBRP	2
99	COMCRP	3
100	COMDRP	4

WHERE S = IS THE LENGTH ALONG THE LINE OF ACTION TO THE POINT OF ENGAGEMENT
AND SO = THE LENGTH OF THE LINE OF ACTION

* *

101	HRTZSP	HERTZ STRESS FOR COMPLIANCE CALCULATION FOR SUN-PLANET
102	HRTZRP	RING-PLANET

** THE PROGRAM WILL USE 101 AND 102 AS CONSTANTS FOR THE COMPLIANCE CALCULATIONS IF INPUT. DEFAULT WILL CALCULATE

```
        THE STATIC LOAD/PITCH RADIUS FOR THE CONSTANTS
103   XPSPSP  IF = 0.0 PLANE STRESS IS ASSUMED FOR SUN-PLANET
              IF = 1.0 PLANE STRAIN IS ASSUMED FOR SUN-PLANET
104   XPSPRP  IF = 0.0       STRESS                RING-PLANET
              IF = 1.0       STRAIN                RING-PLANET

111   CONVEK  IF = 0.0 HELICAL TOOTH IS DIVIDED INTO 10 INDEPENDENT
                      AXIAL SEGMENTS
              IF = 1.0 FINITE ELEMENT ROUTINES USED TO GENERATE AN
                      EQUIVALENT SPUR GEAR COMPLIANCE CURVE
******** FLOATING SUN PARAMETERS ******************************

115   KFSX    LINEAR SPRING IN THE X DIRECTION AT SUN CENTER
116   KFSY    LINEAR SPRING IN THE Y DIRECTION AT SUN CENTER
117   DFSX    LINEAR DAMPER IN THE X DIRECTION AT SUN CENTER
118   DFSY    LINEAR DAMPER IN THE Y DIRECTION AT SUN CENTER
119   FSMS    ACTUAL SUN GEAR MASS (NOT EQUIVALENT MASS)


******* TOOTH PAIR GEOMETRIC DATA ******************************

120   BYPASS IF = 0.0 GEOMETRIC PREPROCESSOR IS USED
             IF = 1.0 GEOMETRIC DATA MUST BE INPUT IN LOCATIONS
                         121-132

121   RADTOS MAX. RADIUS TO BASE OF FILLET OF SUN GEAR      (ROOT
122   RADTOP                                  PLANET GEARS   RADIUS)
123   RADTOR                                  RING GEAR

124   RADTIS MAX. RADIUS TO TIP OF TOOTH OF SUN GEAR
125   RADTIP                                PLANET GEARS
126   RADTIR                                RING GEAR

127   TOOTHS NOMINAL TOOTH THICKNESS AT PD OF SUN GEAR
128   TOOTHP                                  PLANET GEARS
129   TOOTHR                                  RING GEAR

130   RADFIS MAX. FILLET RADIUS OF SUN GEAR
131   RADFIP                       PLANET GEARS
132   RADFIR                       RING GEAR

 ****** FLASH TEMPERATURE DATA *********************************

140   SROU    SURFACE ROUGHNESS (RMS, MICROINCHES)
141   TOIL    OIL INLET TEMPERATURE
142   CFMAT   MATERIAL CONSTANT
143   OILTYP   TYPE OF OIL IN GEARBOX
              1 FOR MIL-L-23699
              2 FOR MIL-L- 7808
              3 TO BE DETERMINED
```

```
            4 TO BE DETERMINED
            (0 DEFAULTS TO TYPE 1)

******* SOLUTION ITERATION DATA ********************************

  150   TOLER    ITERATION TOLERANCE FOR BOUNDARY CONDITION CONVERGENCE
                   (% * 100, DEFAULT FOR LEVEL 1 = .01)
  151   NLOOP    NUMBER OF ITERATIONS FOR BOUNDARY CONDITION CONVERGENCE
                 NLOOP MAXIMUM = 20, DEFAULT = 20.

 ****** TOOTH PAIR GEOMETRIC TOLERANCE DATA ********************

  160   DLROS    TOLERANCE ON TIP RADIUS OF SUN GEAR    (DEFAULT = .002)
  161   DLROP                               PLANET GEARS    "     "    "
  162   DLROR                               RING GEAR       "     "    "
  163   BSE      EDGE BREAK ON TOPLAND OF ALL GEARS     (DEFAULT = .010)
  164   DLRR     ROOT RADIUS TOLERANCE OF ALL GEARS     (DEFAULT = .005)
  165   DLCDN    CENTER DISTANCE TOLERANCE (TOWARD TIGHT MESH)ALL GEARS
  166   DLCDP    CENTER DISTANCE TOLERANCE (AWAY FROM TIGHT MESH)
  167   DLMBT    MACHINE BACKLASH TOLERANCE ALL GEARS   (DEFAULT = .002)

 NOTE:THE TOOTH ROOT FILLET RADIUS TOLERANCE = .005 IN THE PREPROCESSOR

******* 3-DIMENSIONAL FACTORS FOR SPUR GEARS ONLY **************

 * * * * * 175 - 192 NOT REQUIRED FOR LEVEL 2 * * * * * * * * * * * *

  175   SPRNBS   IF = 0. RIM BENDING EFFECTS NOT INCLUDED IN SUN GEAR
                         (DEFAULT = 10.E+10)
                 IF > 0. BENDING SPRINGRATE(IN-#/RAD) OF SUN RIM
  176   SPRNBP   IF = 0. RIM BENDING EFFECTS NOT INCLUDED IN PLANET GEAR
                         (DEFAULT = 10.E+10)
                 IF > 0. BENDING SPRINGRATE(IN-#/RAD) OF PLANET RIM
  177   SPRNBR   IF = 0. RIM BENDING EFFECTS NOT INCLUDED IN RING GEAR
                         (DEFAULT = 10.E+10)
                 IF > 0. BENDING SPRINGRATE(IN-#/RAD) OF RING RIM
  178   SPRNLS   RADIUS FROM RIM TO PD (REQUIRED WITH SPRNBS) SUN
  179   SPRNLP   RADIUS FROM RIM TO PD (REQUIRED WITH SPRNBP) PLANET
  180   SPRNLR   RADIUS FROM RIM TO PD (REQUIRED WITH SPRNBR) PLANET

  181   EFWD1S           EFFECTIVE SUN FACE WIDTH FACTOR AT TOOTH TIP
                 IF = 0. (DEFAULT = 1.0)
  182   EFWD2S           EFFECTIVE SUN FACE WIDTH FACTOR AT FILLET
                 IF = 0. (DEFAULT = 1.0)
  183   EFWD1P           EFFECTIVE PLANET FACE WIDTH FACTOR AT TOOTH TIP
                 IF = 0. (DEFAULT = 1.0)
  184   EFWD2P           EFFECTIVE PLANET FACE WIDTH FACTOR AT FILLET
                 IF = 0. (DEFAULT = 1.0)
  185   EFWD1R           EFFECTIVE RING FACE WIDTH FACTOR AT TOOTH TIP
                 IF = 0. (DEFAULT = 1.0)
```

```
186   EFWD2R          EFFECTIVE RING FACE WIDTH FACTOR AT FILLET
              IF = 0. (DEFAULT = 1.0)
187   STRSES  STRESS DISTRIB. FACTOR FOR END EFFTS AT SUN WIDTH EDGE
              IF = 0. (DEFAULT = 1.0)
188   STRSCS  STRESS DISTRIB. FACTOR FOR END EFFTS AT SUN WIDTH CENT
              IF = 0. (DEFAULT = 1.0)
189   STRSEP  STRESS DISTRIB. FACTOR FOR END EFFTS AT PLAN WDTH EDGE
              IF = 0. (DEFAULT = 1.0)
190   STRSCP  STRESS DISTRIB. FACTOR FOR END EFFTS AT PLAN WDTH CENT
              IF = 0. (DEFAULT = 1.0)
191   STRSER  STRESS DISTRIB. FACTOR FOR END EFFTS AT RING WDTH EDGE
              IF = 0. (DEFAULT = 1.0)
192   STRSCR  STRESS DISTRIB. FACTOR FOR END EFFTS AT RING WDTH CENT
              IF = 0. (DEFAULT = 1.0)

******* HELIX ANGLE ERRORS *************************************

195   DELPSP  HELIX ANGLE ERROR FOR SUN-PLANET MESH

196   DELPRP    "     "     "    "  RING-PLANET MESH

197   DELPS2  IF DBHEL = 0.0 DELPS2 = 0.0
              IF DBHEL = 1.0 DELPS2 = HELIX ANGLE ERROR OF RIGHT
                         HALF OF SUN-PLANET DOUBLE HELICAL GEARS
198   DELPR2  IF DBHEL = 0.0 DELPR2 = 0.0
              IF DBHEL = 1.0 DELPR2 = HELIX ANGLE ERROR OF RIGHT
                         HALF OF RING-PLANET DOUBLE HELICAL GEARS

******* TOOTH PAIR SPACING ERRORS ******************************

200   DR    SUN RUNOUT ERROR FOR EXTERNAL-EXTERNAL SINGLE MESH ONLY
            (K=4), DISPLACEMENT ERROR OF SUN CENTER

    ** NOTE:  A WRITE(7,5029) STATEMENT NEEDS A COMMENT STATEMENT
              REMOVED FOR TIME AND LOADS TO BE OUTPUT, OTHERWISE
              CARDS ARE PUNCHED WHEN A TAPE IS WRITTEN.  IT IS IN
              SUBROUTINE STRESS.


    **NOTE: FOR DOUBLE HELICAL GEARS (DBHEL = 1.0) THE FIRST 10
            VALUES OF I IN THE E(I,J) ARRAYS ARE FOR THE LEFT HALF
            OF THE DOUBLE HELICAL GEARS AND THE LAST 10 LOCATIONS
            ARE FOR THE RIGHT HALF OFTHE DOUBLE HELICAL GEARS,
            WHERE I = THE PLANET NUMBER.

 THE ERRORS SHOULD BE PUT ON THE SECOND OR THIRD TOOTH TO ILLUSTRATE
   THE DYNAMICS.

221 TO 240   ESP(I,1)SUN-PLANET ERROR ARRAY FOR TOOTH 1
241 TO 260   ESP(I,2)                                2
```

```
  261 TO 280   ESP(I,3)                                  3
  281 TO 300   ESP(I,4)                                  4
  301 TO 320   ESP(I,5)                                  5

  321 TO 340   ERP(I,1)RING-PLANET ERROR ARRAY FOR TOOTH 1
  341 TO 360   ERP(I,2)                                  2
  361 TO 380   ERP(I,3)                                  3
  381 TO 400   ERP(I,4)                                  4
  401 TO 420   ERP(I,5)                                  5

******* PLANET GEARS PHASING CONSTANTS ************************

  421 TO 440  KSP(I)   SUN-PLANET PHASING CONSTANTS ARRAY
  441 TO 460  KRP(I)  RING-PLANET PHASING CONSTANTS ARRAY

******* INITIAL BOUNDARY CONDITIONS ***************************

  481 TO 500  XOSP(I)  SUN-PLANET INITIAL DISPLACEMENT BOUNDARY COND
                       OR SUN DISPLACEMENT FOR K=6 OR K=7.
  501 TO 520  XORP(I) RING-PLANET INITIAL DISPLACEMENT BOUNDARY COND
                       OR PLANET DISPLACEMENT FOR K=6 OR K=7.
  521 TO 540  X1SP(I)  SUN-PLANET INITIAL VELOCITY BOUNDARY COND
                       OR SUN VELOCITY FOR K=6 OR K=7.
  541 TO 560  X1RP(I) RING-PLANET INITIAL VELOCITY BOUNDARY COND
                       OR PLANET VELOCITY FOR K=6 OR K=7.

  FLOATING SUN INITIAL  CONDITIONS

  561    CARRIER DISPLACEMENT
  581    CARRIER VELOCITY
  601    RING DISPLACEMENT
  621    RING VELOCITY
  641    SUN CENTER DISPLACEMENT IN X DIRECTION
  642    SUN CENTER DISPLACEMENT IN Y DIRECTION
  643    SUN CENTER VELOCITY IN X DIRECTION
  644    SUN CENTER VELOCITY IN Y DIRECTION

******* PROGRAM PLOT SELECTIONS FOR SPUR GEARS ONLY ************

  651    PLTLD   IF = 0.0
                 IF = 1.0 LOAD PLOTS, NORMALIZED LOAD--DYNAMIC/STATIC
  652    PLTPV   IF = 0.0
                 IF = 1.0 PV   PLOTS, PRESSURE SLIDING VELOCITY
  653    PLTHS   IF = 0.0
                 IF = 1.0 HERTZ STRESS PLOTS
  654    PLTFT   IF = 0.0
                 IF = 1.0 FLASH TEMPERATURE PLOTS
  655    PLTSS   IF = 0.0
                 IF = 1.0 SUN GEAR HEYWOOD STRESS PLOTS
  656    PLTPSS  IF = 0.0
```

```
             IF = 1.0 SUN-PLANET PLANET GEAR HEYWOOD STRESS PLOTS
  657  PLTPRS IF = 0.0
              IF = 1.0 RING-PLANET PLANET GEAR HEYWOOD STRESS PLOTS
  658  PLTRPS IF = 0.0
              IF = 1.0 RING GEAR HEYWOOD STRESS PLOTS

******* PROGRAM CHECK RUN ***************************************

  699  CHECK  IF = 0.0 REGULAR RUN TO COMPLETION
              IF = 1.0 EXITS PROGRAM BEFORE DYNAMIC SOLUTION
                       TO ALLOW CHECKING OF INPUT DATA AND THE
                       GEOMETRIC PREPROCESSOR RESULTS


  * * * * * * * * * * * * * * * * * * * * * * * * * * * * * * * * * * *

 ****** FLEXIBLE PLANET CARRIER OR RING GEAR RIM DATA **********

  800  CARRK1 IF K=6, PLANET CARRIER STIFFNESS ALONG-THE-LINE-OF-
                      ACTION (#/IN)

  801  CARRK2 IF K=7 RING GEAR RIM STIFFNESS ALONG-THE-LINE-OF-
              ACTION (#/IN)
  802  KFLX1  PLANET/CARRIER 'PIN' OR  INTERFACE STIFFNESS
  803  KFLX2  PLANET/RING 'PIN' OR INTERFACE STIFFNESS

*********************  NATURAL FREQUENCIES OPTION *****************

  805  NFREQ  TRIGGER FOR NATURAL FREQUENCY OPTION
              = 1, OUTPUTS FREQUENCIES IN TERMS OF INPUT RPM
              = 2, OUTPUTS FREQUENCIES IN TERMS OF INPUT RPM
                   AS WELL AS THE FREQUENCIES WITH EIGENVECTORS

           ** SEE USER'S MANUAL IN 1986 CR FOR ADDITIONAL SYSTEM
              TYPES THAT ARE AVAILABLE
```

***** OUTPUT DESCRIPTION

THE FOLLOWING LIST INDICATES THE INFORMATION AND RESULTS THAT MAY APPEAR IN THE OUTPUT, IN THE ORDER THEY WILL APPEAR.

CASE TITLE—THE TITLE AND/OR OTHER INFORMATION INPUT ON THE FIRST DATA CARD.

TIP MODIFICATION—IF THERE IS INSUFFICIENT TIP CLEARANCE, AN ADJUSTMENT IS MADE INTERNALLY AND A MESSAGE OUTPUT UNTIL SUFFICIENT CLEARANCE IF OBTAINED.

INVOLUTE MODIFICATION TABLE—SHOWS THE PROCESSED RESULTS OF ANY INPUT PROFILE MODIFICATIONS. TABLES ARE PRINTED FOR ENGAGEMENT AND DISENGAGEMENT WHICH INCLUDE MINIMUM AND MAXIMUM INVOLUTE MODIFICATIONS, DIAMETER AND CORRESPONDING ROLL ANGLE FOR THE MODIFIED PORTION OF THE PROFILE. THIS WILL BE OUTPUT FOR THE SUN-PLANET MESH AND/OR RING-PLANET MESH IN CONJUNCTION WITH THE CORRESPONDING INPUT DATA.

INPUT DATA—THE INPUT DATA AND PREPROCESSED GEOMETRIC DATA IS PRINTED FOR SUN-PLANET MESH AND/OR RING-PLANET MESH.

FLEXIBILITY—IF THE FLEXIBLE PLANET CARRIER OPTION IS IN EFFECT A MESSAGE APPEARS THAT INDICATES THIS.

ADDITIONAL INPUT DATA—NUMBER OF PLANETS, EQUIVALENT MASSES, ETC.

COMPLIANCE CONSTANTS—CALCULATED CONSTANTS FOR FOURTH ORDER COMPLIANCE EQUATION.

ITERATED BOUNDARY CONDITIONS—BOUNDARY CONDITIONS PRINTED, FOLLOWED BY THE CURRENT SPEED BEING EXAMINED AND CORRESPONDING MAXIMUM LOADS (FOR SUN-PLANET AND/OR RING-PLANET MESHES).
IF A SPEED SURVEY WAS RUN, THE SPEED CORRESPONDING TO THE OVERALL MAXIMUM LOAD FROM THE RANGE CALCULATED IS OUTPUT WITH THE MAXIMUM LOAD. THIS IS THE SPEED USED FOR THE REMAINING CALCULATIONS, I.E. STRESS.

MAXIMUM VALUES—TABLE(S) OF MAXIMUM VALUES CALCULATED ARE PRINTED FOR EACH SUN-PLANET MESH AND/OR RING-PLANET MESH. THESE WILL APPEAR FOR THE NO ERROR SOLUTION AND EACH ERROR SOLUTION. TWO ABBREVIATIONS APPEAR—PV=PRESSURE SLIDING VELOCITY AND PD=PITCH DIAMETER.

ERROR MATRIX—IF TOOTH SPACING ERRORS ARE INPUT, OR GENERATED FOR RUNOUT SOLUTION, A TABLE OF ERRORS IS PRINTED BEFORE THE TABLES OF MAXIMUM VALUES.

PLOTS — WILL BE FOR EACH PLANET MESH.

IF THERE ARE TOOTH PAIR SPACING ERRORS INCLUDED,PLOTS ARE GENERATED FOR THE NO ERROR CASE ONLY , I.E. THERE ARE NO PLOTS GENERATED FOR THE ERROR CASES.

APPENDIX B: FIRST ORDER DIFFERENTIAL EQUATIONS

A. Floating Sun Equations:

The equations can be transformed to first order equations as follows.

Let:

$$
\begin{aligned}
\dot{x}_1 &= \ddot{x} & \dot{x}_3 &= \ddot{y} \\
\dot{x}_2 &= x_1 = \dot{x} & \dot{x}_4 &= x_3 = \dot{y} \\
\dot{x}_5 &= \ddot{y}_c & \dot{x}_7 &= \ddot{y}_r \\
\dot{x}_6 &= \dot{y}_c = x_5 & \dot{x}_8 &= \dot{y}_r = x_7
\end{aligned}
\tag{1}
$$

$$
\begin{aligned}
\dot{x}_1 = \frac{1}{m_s} \Big[&\sum_{i=1}^{N} d_{sp_i} \dot{y}_{sp_i} \sin \alpha_i + \sum_{i=1}^{N} L_{sp_i} \sin \alpha_i \\
&- d_x x_1 - k_x x_2 \Big]
\end{aligned}
\tag{2a}
$$

$$
\dot{x}_2 = x_1 \tag{2b}
$$

$$
\begin{aligned}
\dot{x}_3 = -\frac{1}{m_s} \Big[&\sum_{i=1}^{N} d_{sp_i} \dot{y}_{sp_i} \cos \alpha_i + \sum_{i=1}^{N} L_{sp_i} \cos \alpha_i \\
&+ d_y x_3 + k_y x_4 \Big]
\end{aligned}
\tag{3a}
$$

$$
\dot{x}_4 = x_3 \tag{3b}
$$

$$
\begin{aligned}
\dot{x}_5 = \frac{1}{m_c} \Big[&\sum_{i=1}^{N} d_{sp_i} \dot{y}_{sp_i} + \sum_{i=1}^{N} d_{rp_i} \dot{y}_{rp_i} \\
&+ \sum_{i=1}^{N} L_{sp_i} + \sum_{i=1}^{N} L_{rp_i} + F_c \Big]
\end{aligned}
\tag{4a}
$$

$$
\dot{x}_6 = x_5 \tag{4b}
$$

$$
\dot{x}_7 = \frac{1}{m_r} \Big[\sum_{i=1}^{N} d_{rp_i} \dot{y}_{rp_i} + \sum_{i=1}^{N} L_{rp_i} + F_r \Big] \tag{5a}
$$

$$
\dot{x}_8 = x_7 \tag{5b}
$$

B. Flexible Carrier Equations

The carrier and ring gear equations are reduced to first order equations as follows.

Let

$$x_{c_{i0}} = y_{c_i} \qquad (6a)$$

$$x_{c_{i1}} = \dot{y}_{c_i} \qquad (6b)$$

$$\dot{x}_{c_{i1}} = \ddot{y}_{c_i} \qquad (6c)$$

$$\begin{aligned} \dot{x}_{c_{i1}} = {} & \frac{1}{m_{c_i}} d_{sp_i}(x_{s_i} - x_{p_{i1}} - x_{c_{i1}}) - \frac{1}{m_{c_i}} d_{rp_i}(x_{p_{i1}} - x_{c_{i1}} - x_{r_{i1}}) \\ & - \frac{1}{m_{c_i}} L_{sp_i} - \frac{1}{m_{c_i}} L_{rp_i} + \frac{K_c}{m_{c_i}}(x_{c_{i0}} - x_{c_{i+1_0}}) + \frac{K_{c_{i-1}}}{m_{c_{i-1}}}(-x_{c_{i-1}} + x_{c_{i0}}) \\ & = -\tau_{out_c}/m_{c_i} N R_{b_c} \end{aligned} \qquad (7)$$

(carrier)

$$\dot{x}_{c_{i0}} = x_{c_{i1}}$$

Let

$$x_{r_{i0}} = y_{r_i} \qquad (8a)$$

$$x_{r_{i1}} = \dot{y}_{r_i} \qquad (8b)$$

$$\dot{x}_{r_{i1}} = \ddot{y}_{r_i} \qquad (8c)$$

$$\begin{aligned} \dot{x}_{r_{i1}} - {} & \frac{1}{m_{r_i}} d_{rp_i}(x_{p_{i1}} - x_{c_{i1}} - x_{r_{i1}}) - \frac{1}{m_{r_i}} L_{rp_i} \\ & + \frac{1}{m_{r_{i-1}}} k_{r_{i-1}}(-x_{r_{i-1_0}} + x_{r_{i_0}}) + \frac{1}{m_{r_i}} K_{r_i}(x_{r_{i_0}} - x_{r_{i+1_0}}) \\ & = -\tau_{out_r} / m_{r_i} N R_{b_r} \end{aligned} \qquad (9)$$

(ring)

$$\dot{x}_{r_{i0}} = x_{r_{i1}}$$

The equation for the torque constraint reduces as follows.

Let

$$Z = x \tag{10a}$$

$$\dot{Z} = \dot{x} = R \tag{10b}$$

$$\ddot{Z} = \ddot{x} = \dot{R} \tag{10c}$$

$$R = \dot{x} \tag{10d}$$

$$\dot{R} = (\tau_{out} / R_{b_c} - \sum_{i=1}^{N} K_c Y_{c_i}) / M \tag{11}$$

APPENDIX C: FORTRAN LISTING

The program listing is available from NASA Project Manager or Contractor upon request.

APPENDIX D: NOMENCLATURE

A,B,C,D = gear tooth coefficients

C = single tooth pair compliance (in/lb)

C_o = single tooth pair compliance at pitch radius (Reciprocal of spring rate) (in/lb)

d_{rp_i} = ring-planet tooth pair damping (lb s/in)

d_{sp_i} = sun-planet tooth pair damping (lb s/in)

d_x = damping at sun center in x-direction (lb s/in)

d_y = damping at sun center in y-direction (lb s/in)

$e_{rp_{ij}}$ = tooth spacing error, ring-planet mesh

$e_{sp_{ij}}$ = tooth spacing error, sun-planet mesh

f_I = gear mesh frequencies

I = integer multiplier of gear mesh frequencies

$[K]$ = stiffness matrix (lb/in)

$\bar{K}_{c_i}$ = planet/carrier pin stiffness (lb/in)

K_{c_i} = carrier segment stiffness (lb/in)

$\bar{K}_{r_i}$ = planet/ring stiffness (lb/in)

K_{r_i} = ring gear rim segment stiffness (lb/in)

k_{rp_i} = ring-planet tooth pair stiffness (lb/in)

k_{sp_i} = sun-planet tooth pair stiffness (lb/in)

k_x = spring rate at sun center in x-direction (lb/in)

k_y = spring rate at sun center in y-direction (lb/in)

L_{rp_i} = ring-planet tooth pair load for planet mesh i

L_{sp_i} = sun-planet tooth pair load for planet mesh i

[M] = mass matrix, a diagonal matrix (lb.)

M = artificial mass for total torque constraint

m = translational mass of the sun gear (lbs s**2/in)

m_c = rotational (equivalent) mass of the planet carrier (lbs s**2/in)

m_r = rotational (equivalent) mass of the ring gear (lbs s**2/in)

N = number of planets

R_{b_c} = Carrier Base Radius (in)

R_{b_r} = Ring Gear Base Radius (in)

rpm = speed of driving gear

S = motion along line of action from pitch line

S_o = Reference distance along line of contact for tooth pair dompliance coefficients

x = displacement of the sun center in x-direction (in)

X_{LOA_i} = Sun-planet displacment along the line of action due to the floating sun (in)

XN = Number of teeth on driver

Y = displacement of the sun center in y-direction (in)

Y_{rp_i} = ring-planet tooth pair displacement for planet mesh i

Y_{sp_i} = sun-planet tooth pair displacement for planet mesh i

α_i = $\theta_c + \psi_i - \Phi$ (planetary)

α_i = $\psi_i - \Phi - \theta_r$ (star)

$\beta_{rp_{ji}}$ = Cam modification, ring-planet mesh

$\beta_{sp_{ji}}$ = Cam modification, sun-planet mesh

η_{rp_i} = Ring-Planet tooth pair spring rates

η_{sp_i} = Sun-Planet tooth pair spring rates

θ_c = carrier angle of rotation

θ_r = ring angle of rotation

λ = ω^2

τ_{out} = Output Torque

Φ = pressure angle

$\phi_{rp_{ji}}$ = Identify function for ring-planet tooth pair contact

$\phi_{sp_{ji}}$ = Identify function for sun-planet tooth pair contact

ψ_i = relative angular position of planets
= $2\pi(i-1)/N$, $i = 1,2,3,\ldots N$

ω = natural frequency (rad/s)

$\chi_{sp_{ji}}$ = 0 or 1 depending on whether the tooth contact is on the profile modification cam or not

Subscripts

c = carrier

i = planet mesh

j = tooth pair mesh

p = planet gear

r = ring gear

s = sun gear